Archaeological and Anthropological Sciences (2025) 17:58
https://doi.org/10.1007/s12520-024-02147-6

RESEARCH

Multi-isotopic evidence reveals the emergence of a cosmopolitan community at the Luistari cemetery in Eura, Finland, during the early Medieval period (600–1130 CE)

Alžběta Danielisová[1] · Ulla Nordfors[2] · Samuel Kertes[1] · Anna Wessman[3] · Lukáš Ackerman[4] · Markku Oinonen[5] · Heli Etu-Sihvola[5] · Laura Arppe[5]

Received: 7 June 2024 / Accepted: 16 December 2024

Abstract

This study examines the role of the Eura region as a nexus linking the inland with Baltic Sea trade routes. Luistari cemetery, spanning from the early Merovingian to Medieval periods, provides key insights into South-Western Finland's socio-economic structure and communication networks. Despite its significance, this burial community's chronological dynamics and regional role remain poorly understood. Using multi-isotopic evidence contextualised with archaeological data, this research explores mobility and subsistence patterns among Luistari's population. By delineating the bioavailable strontium range in the Eura region, the study assesses the local burial community's mobility dynamics across various chronological phases. Identification of long- and short-distance migrants, discerned through strontium and carbon isotopes in conjunction with archaeological context, enhances understanding of Luistari within the regional and Circum-Baltic framework. Multi-isotopic evidence further aids in grasping local development within environmental and climatic contexts. Analysis of the strontium isotopic data patterns, combined with carbon and nitrogen, sheds light on settlement locations and subsistence strategies of the Luistari population. Notable transformations during the Viking I period (800–880 CE), marked by the establishment of a "founding" community, and shifts in dietary and migratory patterns in periods V II-III (880–1000 CE), indicate stabilisation of the local socio-economic conditions. Period V IV (1000–1070 CE) reveals connections, both maritime and continental, as the local community integrates into long-distance communication networks. The Final Period (1070–1130 CE) then shows only limited signs of mobility. The data suggest varied mobility patterns over the long-term development of the local community coupled with visibly changing subsistence strategies.

Keywords Circum-baltic area · Viking age · Strontium · Stable isotopes · Mobility · Food catchments

✉ Alžběta Danielisová
danielisova@arup.cas.cz

✉ Laura Arppe
laura.arppe@helsinki.fi

Ulla Nordfors
ummoil@utu.fi

Samuel Kertes
kertes@arup.cas.cz

Anna Wessman
anna.wessman@uib.no

Lukáš Ackerman
ackerman@gli.cas.cz

Markku Oinonen
markku.j.oinonen@helsinki.fi

Heli Etu-Sihvola
heli.etu-sihvola@helsinki.fi

[1] Institute of Archaeology of the CAS, Prague, Czech Republic

[2] University of Turku, Turku, Finland

[3] University of Bergen, Bergen, Norway

[4] Institute of Geology of the CAS, Prague, Czech Republic

[5] Finnish Museum of Natural History, University of Helsinki, Helsinki, Finland

Published online: 08 February 2025

Introduction

The coastal regions of Finland are closely tied to the broader socio-economic developments around the Baltic Sea during the Viking Age (Fig. 1). Archaeological evidence indicates extensive interactions across the sea; objects originating from Scandinavia, the Baltic region, and even more distant locations have been found in Finland, while materials of Finnish origin have been identified in Sweden (Kivikoski 1937; Gustin 2017). Trade, particularly the exchange of furs and other outland products (e.g. Callmer 2024; Hennius 2021; Stene and Wangen 2017), has been seen as a significant factor shaping the Viking Age societies across Northern Europe, and the expansion of trade networks contributed significantly to the economic growth throughout the region in the era (e.g. Sindbæk and Arthur 2008; Gustin 2017; Gustin and Wessman 2021). The municipality of Eura is located between the Finnish coast (Fig. 1) and the dense coniferous forests of the inland, and the position likely made it a crucial nexus linking the inland sources of luxurious fur products with the maritime trade networks of the Baltic Sea already during the Iron Age (Kivikoski 1964: 215–216 Lehtosalo-Hilander 1982a: 74; Raninen and Wessman 2015: 329–334). This suggests that Eura may have played a vital role in facilitating trade and exchange between the interior regions rich in fur resources and the sea trading routes.

The inhumation cemetery of Luistari in Eura was established in the early Merovingian Period (late 6th century

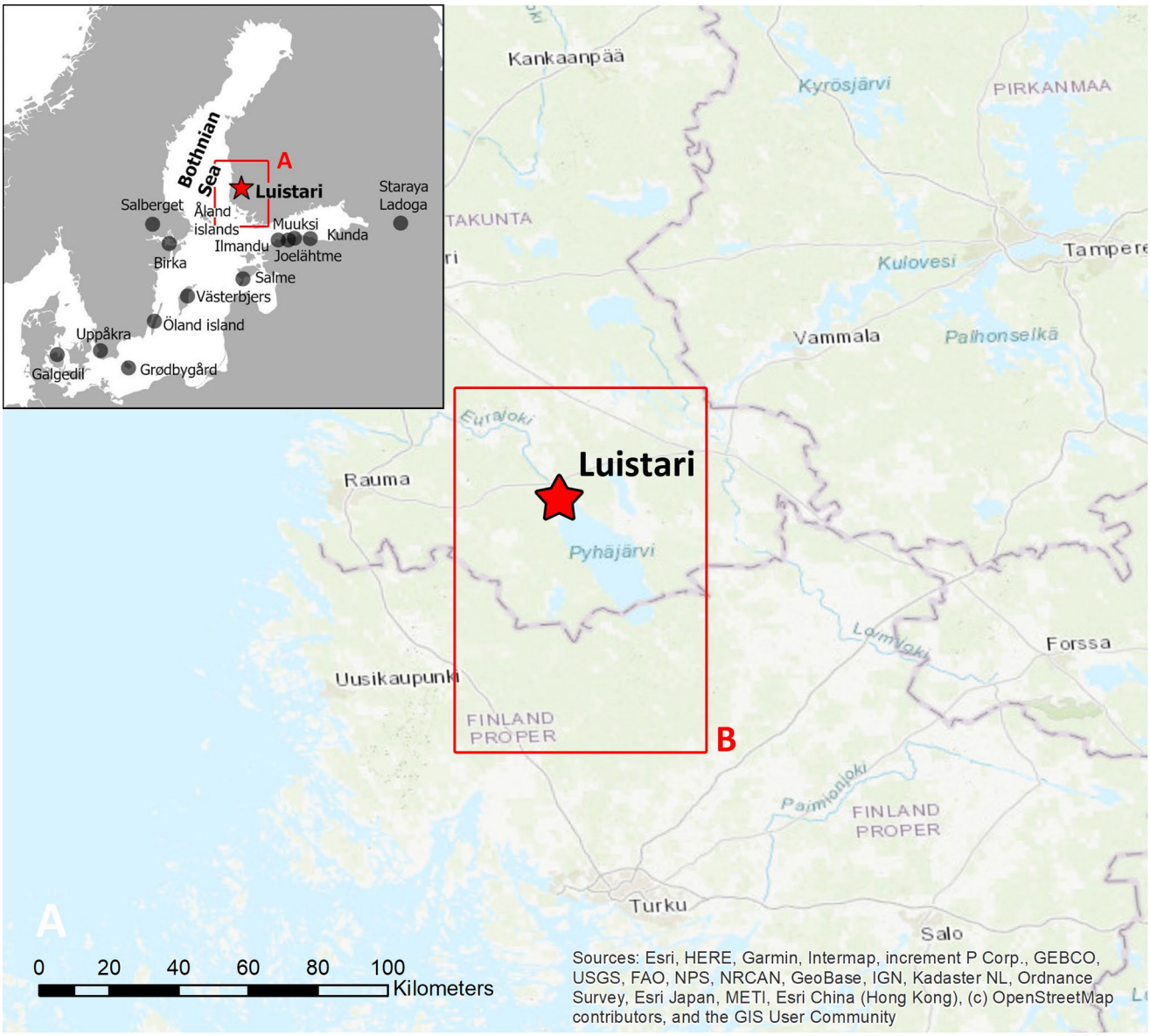

Fig. 1 Circum-Baltic area with the archaeological sites mentioned in the text. Southwestern Finland (**A**) with the study area around Luistari indicated (**B**)

CE), and it was continuously used through the Viking Age (c. 800–1050 CE) until the Medieval Period (c. 14th century CE) (Lehtosalo-Hilander 1982a-; 1982b; 1982c; 2000). With its 1300 graves, Luistari is one of the largest known inhumation cemeteries in the Nordic countries, and studies of the graves and artefacts have produced significant knowledge on the Iron Age and Early Medieval period of South-Western Finland, including material culture, social and economic patterns and contacts. Luistari stands out as a crucial source of information of the period, since contemporary settlement sites from the area have not been excavated, and their exact locations in relation to the cemetery remain unknown. Despite its importance as a hub in the Nordic cultural, economic, and political network, little has been understood about the Luistari burial community, particularly regarding its internal structure and active role and position in the circum-Baltic area in relation to temporal dynamics of the site. Furthermore, because of the lack of settlement evidence, insights into the subsistence strategies of the local community have been limited in extent (e.g. Kirkinen et al. 2020), the most comprehensive so far being a recent study on dietary isotope analysis (Etu-Sihvola et al. 2022).

By utilising multi-isotopic (Sr, O, C and N) evidence alongside archaeological data, our aim is to explore various aspects relevant to mobility, settlement and subsistence of the early Medieval burial population of the Luistari cemetery. By delineating the bioavailable strontium range in the Eura region, we assess the mobility dynamics of the local burial community across different chronological phases. Furthermore, the identification of long-distance migrants (i.e. incomers from areas beyond the Eura region), discernible through the combination of strontium isotopes with other isotopic evidence and archaeological contextualisation, sheds light on the character of the Luistari community within the context of early Medieval sites in the Circum-Baltic area. This aids in contextualising this community within the historical development at the supra-regional level. Community development, as reflected in multi-isotopic patterns, is also evaluated against environmental and climatic conditions which underwent changes that may or may not have influenced the evolving local community. The specific variations of the isotopic data shed light on potential settlement patterns, with differing food catchments among individual groups within the Luistari community, and their subsistence strategies from the beginning of the cemetery to the final period of the local community's evolution.

Isotope provenancing in mobility research

The differentiation between locals and non-locals forms the basis for reconstructing population mobility dynamics and understanding its significance in shaping socioeconomic, cultural, and political connections. Mobility isotope tracers, particularly strontium and oxygen, are employed to ascertain the origin of samples by comparing their isotopic composition with the local background.

Strontium, a common trace element found in nature, serves as a valuable tool in provenance analysis due to its variable presence in geologically distinct rocks. The discriminative value of the radiogenic $^{87}Sr/^{86}Sr$ ratio, commonly used in analysis, stems from the fact that ^{87}Sr isotope is derived from the radioactive decay of ^{87}Rb, with varying Rb/Sr ratios and ages across geological units (Bentley 2006; Szostek et al. 2015). Older rocks and/or those with high Rb/Sr ratios exhibit highly radiogenic $^{87}Sr/^{86}Sr$ ratios (>0.730), whereas younger rocks or those with very low Rb/Sr (e.g. carbonates) display lower $^{87}Sr/^{86}Sr$ ratios (<0.710), (Montgomery 2010; Sjögren et al. 2016).

Strontium enters the environment through the weathering of bedrock, with the strontium ratios of the parent material reflected in the sedimentary and soil cover. Organisms that consume local water, feed on local bedrock, and breathe local air acquire contemporary strontium isotope composition from the surrounding bioavailable strontium pool, predominantly originating from the bedrock. Thus, strontium serves as an effective tracer due to its minimal fractionation between the geological background and the final consumers of foodstuffs sourced from this background (Bentley 2006; Szostek et al. 2015; Montgomery 2010). Consequently, $^{87}Sr/^{86}Sr$ ratios measured in samples reflect the strontium geology of local food sources. However, the bioavailable strontium pool comprises various components, including sediments of different compositions, such as alluvial, aeolian, or glacial deposits as well as soil and riverine inputs. Factors like sea spray or rainfall in coastal areas also influence the creation of the local bioavailable range (Price et al. 2002; Maurer et al. 2012; Sjögren et al. 2016). Therefore, ensuring an accurate local bioavailable strontium range requires careful consideration. This is typically achieved through sampling of local bedrocks, sediments, plants, and waters, although potential modern contamination can introduce bias into the local signal. In this respect, areas with fertilised soils, in particular, should be sampled cautiously. Organisms with limited mobility ranges, such as small modern fauna, are commonly selected for sampling. When available, archaeological fauna, particularly non-migratory wild species with broadly similar home ranges as humans, often provide the most reliable data (Lengfelder et al. 2019; Szostek et al. 2015; Holt et al. 2021).

In living organisms, specifically humans and animals, strontium is largely hosted by the hydroxyapatite - a calcium phosphate mineral forming an inorganic fraction of teeth and bones, where Sr substitutes for calcium. Enamel is typically the preferred tissue for sampling in provenance

studies due to its robust preservation and resistance to diagenesis (Montgomery 2010; Bentley 2006). While archaeological bones are not ideal for mobility studies due to their susceptibility to soil contamination, they can still provide useful insights into the local bio-available strontium signal. Enamel, however, only reflects the childhood origin of the sample and does not provide information on adult mobility due to its resistance to modify primary Sr isotopic signature (Bentley 2006; Montgomery 2010; Sjögren et al. 2016). To address this limitation, other isotopic systems, such as sulphur, can be utilised (Bataille et al. 2021). Additionally, insights into sulphur-based mobility can be gleaned from isotopic differences between the childhood signal preserved in dentine and the adult signal from bones, which undergo turnover over several years (Fahy et al. 2017).

In mobility studies, strontium is often paired with oxygen isotope systematics ($\delta^{18}O$), providing insights into the relationship between food catchments and water sources that organisms ingest (Lightfoot and O'Connell 2016), essentially linking geology with climate. Oxygen exhibits less geographical variation compared to strontium, especially in temperate regions (Budd et al. 2004). At the same time, intra-population variability in $\delta^{18}O$ values can be significant, usually always larger than 3‰ and reaching up to 8‰ due to anthropological manipulation of water sources and various physiological processes (Lightfoot and O'Connell 2016). Consequently, the statistical significance for identifying migrants especially in smaller population samples is much lower compared e.g. to Sr, and pinpointing specific regions of origin becomes challenging (Lightfoot and O'Connell 2016), making oxygen isotope compositions alone less conducive for provenance analysis. However, when combined with radiogenic strontium and other stable isotopes, i.e. carbon, nitrogen and sulphur (e.g., Bataille et al. 2021; Sjögren et al. 2016; Velte et al. 2023; Knipper et al. 2020), the multi-isotopic evidence proves to be quite effective in the mobility studies of living organisms.

Geographical and geological background of Luistari

The site is situated north from the shore of the large (155.2 km^2) lake Pyhäjärvi (Fig. 1), supporting abundant fish stocks and water fowls. The lake is fed by two larger rivers, Yläneenjoki with catchments (233 km^2) in the south-southeast, and Pyhäjoki gathering waters from watersheds (77 km^2) to the east. The area is connected to the Baltic Sea through the outlet river Eurajoki flowing 53 km to the north-northwest to the Gulf of Bothnia. Furthermore, the area is within an easy travel distance from river Kokemäenjoki, one of the major waterways connecting the Baltic sea to the inland regions of Pirkanmaa and Häme further to the southeast.

The bedrock of the Eura area presents interesting contrasts in rock composition (Kohonen 1993) (Fig. 2A). The Eurajoki river flows at the contact of the Mesoproterozoic Laitila Rapakivi granite massif (Vaasjoki 1977; 1.59–1.54 Ga) and the Satakunta sandstone (Kohonen 1993; 1.6–1.3 Ga), the latter making up the entire basement of lake Pyhäjärvi. The sandstone is an uncommon rock unit in Finland (Nironen 2017). It contains calcite as diagenetic cement, interlayers and concretions, also dispersed into the glaciogenic sediments and aquifers of the region (Kortelainen et al. 2007). In addition to the Rapakivi granite and the sandstone, associated with 1.27 Ga diabase, the bedrock to the east and south of lake Pyhäjärvi is comprised of Paleoproterozoic igneous and metamorphic rocks, consisting mainly of 1.88–1.87 Ga granodiorite, quartz diorite and tonalite, and 1.91–1.88 Ga biotite paragneiss with occurrences of metavolcanic and volcaniclastic rocks (amphibolite and hornblende gneiss, respectively)(see review by Lehtinen et al. 2005). For simplicity, the Paleoproterozoic bedrock units are referred to as "eastern felsic rocks" (granodiorite, quartz diorite and tonalite) and "southern metamorphic rocks" (paragneiss, metavolcanic and volcaniclastic rocks) later in the text.

The crystalline bedrock is overlain by a variable cover of loose Quaternary deposits. The Quaternary cover can be split into two contrasting sectors along a NW-SE trending transect running through lake Pyhäjärvi (Fig. 2B). To the west and south of this divide, ca. 50% of the terrain is exposed bedrock surface or bedrock covered with less than 1 m of loose sediment, while the other 50% is covered by till, peat deposits and clays up to 10 m thick. To the north and east of this divide, the much thicker Quaternary cover is made up in roughly equal proportions of clay and silt deposits, till and glaciofluvial deposits like littoral sands and silts as well as ice marginal formations, generally 10–30 m, but up to 88 m thick in the core of the Säkylänharju-Virttaankangas interlobate esker formation. Thus, much of the Rapakivi granite as well as the southern metamorphic rocks are exposed or thinly covered, while the areas underlain by Satakunta sandstone and the eastern felsic rocks are under a thicker cover of Quaternary deposits.

Materials and methods

Materials

The Iron Age chronology of Luistari cemetery has been divided into several phases based on artefact typology: Merovingian I (**M I**, 600–750 CE), Merovingian II (**M II**, 750–800 CE), Early Viking (**V I** 800–880 CE), Mid Viking (**V II-III**, 880–1000 CE), Later Viking II (**V IV**, 1000–1070 CE), and the Final Period (**FP**, 1070–1130

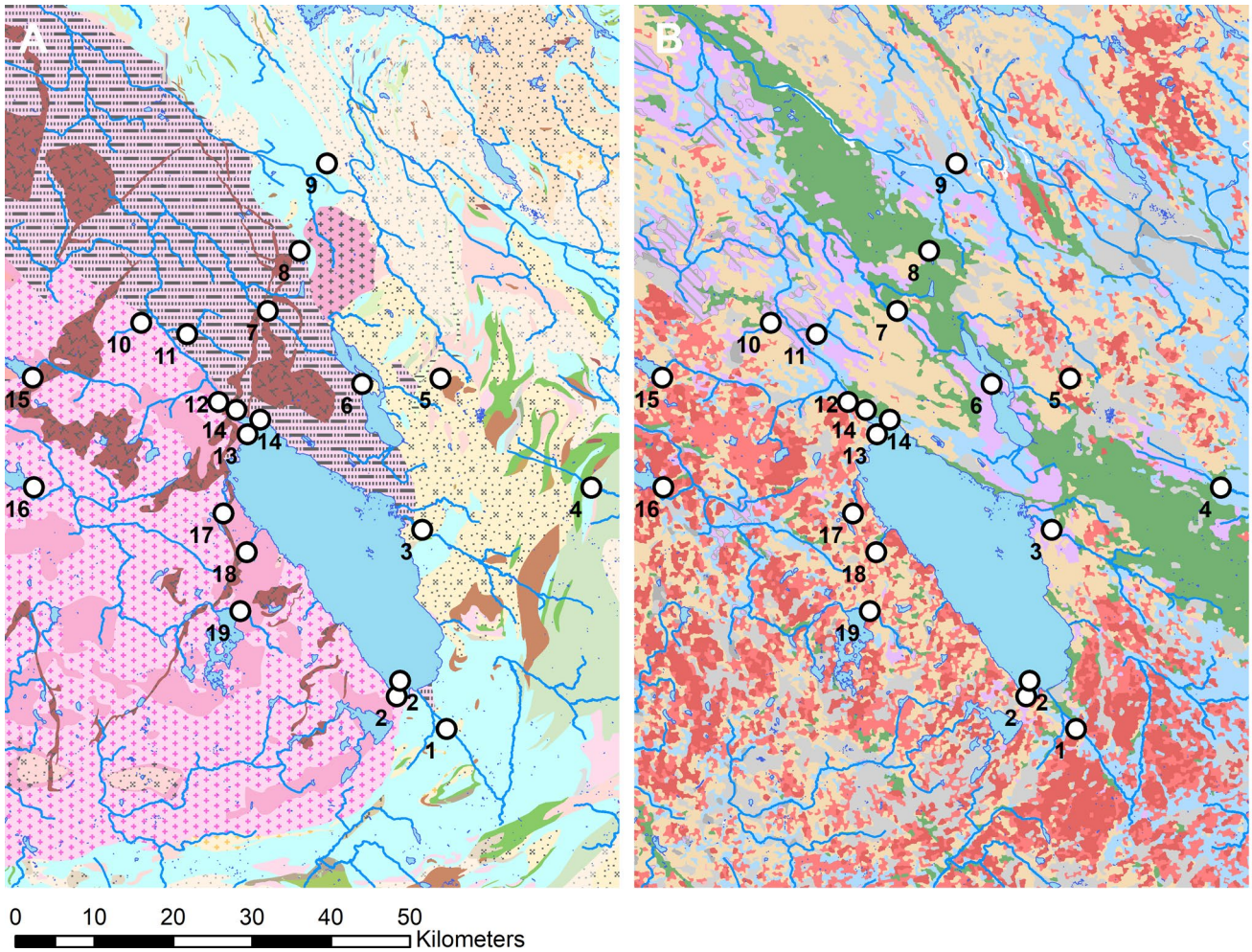

Fig. 2 Geological bedrock map (**A**), and surficial Quaternary deposits map (**B**) of the Eurajoki area with bioavailable strontium sampling sites projected. Sampling site 12 is the Luistari cemetery. For details on samples see Supplementary Table 2; for legend of geological units and surficial deposit units see Supplementary Information 2. Data sources: Bedrock of Finland 1:200 000 (**A**) and Superficial deposits of Finland 1:200 000 (**B**) from the Geological Survey of Finland GTK. River network dataset from the Finnish Environment institute SYKE

CE), (Lehtosalo-Hilander 1982b: 173–188; 1982c: 7). New radiocarbon analyses on the Luistari individuals (Etu-Sihvola et al., in preparation) are more or less consistent with the archaeological chronologies. Most (72%) of the dates temporally overlap with the assumed chronological period while the rest are somewhat younger, the possible reasons being poor collagen preservation in non-dental bones and/or overlying younger graves.

The selection of teeth for enamel sampling for strontium and oxygen isotope analysis was significantly influenced by the condition of the osteological remains. Although the cemetery contains over 1300 graves, human remains were only catalogued from 195 of them (Etu-Sihvola et al. 2022). These remains were utilised for enamel sampling for strontium and oxygen isotope analysis (Table 1, Supplementary Fig. 1). In cases where enamel was not preserved but temporal bone was available, *pars petrosa* (indicative about ca. first year of life, cf. Veselka et al. 2021), generally recognized for its outstanding preservation potential (Kootker and Laffoon 2020; Pinhasi et al. 2015), was sampled instead (Supplementary Table 1). Consequently, enamel or *pars petrosa* samples were obtained from 79 individuals. Enamel sampling was conducted using a dental drill after repeated sonication in MilliQ water. In instances where enamel was the only preserved skeletal material in the grave, enamel pieces were collected intact, cleaned by sonication in MilliQ water, and subsequently powdered using an agate mortar. The target sample size aimed for approximately 20 mg of powder material. The primary objective was to ensure a balanced representation across all chronological periods and biological groups.

In case of exceptionally well preserved dentition where it was certain that teeth were coming from a particular individual, samples were collected from multiple teeth (usually M1, PM, M2, and M3) to be able to analyse mobility patterns of individuals in greater detail. Of these multiply-sampled

Table 1 Representation of the individual chronological phases by the Luistari cemetery samples

Period	Type (determination)	Sample count $^{87}Sr/^{86}Sr$	Sample count $\delta^{18}O_p$	Sample count $\delta^{13}C_c$
M I+II	*Males*	2	2	2
	Females	10	9	7
	Children	1	1	1
	Undetermined			
	Total	*13*	*12*	*10*
V I	*Males*	3	3	3
	Females	7	7	5
	Children	1	1	1
	Undetermined	2	2	2
	Total	*13*	*13*	*11*
V II-III	*Males*	11	11	11
	Females	15	15	14
	Children	2	2	1
	Undetermined	2	2	1
	Total	*30*	*30*	*27*
V IV	*Males*	9	9	9
	Females	4	4	4
	Children	2	2	2
	Undetermined			
	Total	*15*	*15*	*15*
FP	*Males*	5	5	4
	Females	3	3	3
	Children			
	Undetermined			
	Total	*8*	*8*	*7*
Animals	*Cattle*	3	5	5
	Sheep/Goats	5	5	5
	Dogs	4	4	

individuals ($n=11$), six were determined as females, four were males and one undetermined (Supplementary Table 1). In case of animal samples, availability and preservation of the enamel were the most driving factors for their selection. In the end, only four cattle and four sheep/goat samples fulfilled the selection criteria (Supplementary Table 1). Four samples of dog enamels (Table 1) followed the same selection process and tried to match the analyses of graves where they were found (Supplementary Table 1).

With no archaeological wild animal enamels available for sampling, the typical levels of bioavailable $^{87}Sr/^{86}Sr$ values in the local environment were surveyed by sampling plants and surface waters (e.g. Szostek et al. 2015; Maurer et al. 2012; Blank et al. 2018; Ladegaard-Pedersen et al. 2021) within an area of ca. 40 km W-E and 45 km N-S centering around the northern shore of lake Pyhäjärvi (Fig. 2, Supplementary Table 2). A total of 36 water and plant samples were collected. Of the waters ($n=17$), eight were taken from lakes and nine from rivers and streams. The plant samples ($n=19$) were mainly leaves of deciduous trees ($n=17$) but at two sites, also berries were collected for analysis. In addition to the plants and waters, three samples of fish caught from lake Pyhäjärvi were analysed. Samples were collected from altogether 19 sites of which 15 are represented by samples of both water and plants. About half of the samples were collected from sites underlain by the Laitila Rapakivi granite, while the Satakunta sandstone, the eastern felsic and southern metamorphic rocks are represented by 11 to five samples each (Table 2). An effort was made to avoid sampling at agricultural areas, as there is active farming, cultivation and forestry in the region, which might exert an influence on the bioavailable $^{87}Sr/^{86}Sr$ pool e.g. through liming (Andreasen and Thomsen 2021). Based on land cover/use classification by the Finnish Environment Institute (SYKE/CORINE Land cover 2012), on average 18% of the catchment areas of the sampled surface waters are categorised as agricultural land, whereas forests, semi natural areas, wetlands and water bodies make up ca. 78% of land cover. Details of the collected samples, including land cover/use shares in the catchment for water sampling sites, are listed in Supplementary Table 2. In addition to the environmental samples, the immediate diagenetic $^{87}Sr/^{86}Sr$ signal of the burial soil was constrained by analysis of nine specimens of archaeological human bone.

Waters were sampled to 100 ml acid-cleaned HDPE bottles through 0.46 µm membrane filter and 0.5 ml ultrapure HNO_3 (Sr, Rb < 0.01 ppt) was added to avoid precipitation of solids and stall biological activity. The samples were

Table 2 The $^{87}Sr/^{86}Sr$ ratios of the water and plant samples categorised according to the underlying bedrock

Bedrock type	$^{87}Sr/^{86}Sr$ plant samples				$^{87}Sr/^{86}Sr$ water samples			
	Range	Mean	Median	*n*	Range	Mean	Median	*n*
Rapakivi granite	0.7218-0.7734	0.7386	0.7372	9	0.7252-0.7384	0.7324	0.7337	6
Satakunta sandstone	0.7297-0.7385	0.7333	0.7325	4	0.7204-0.7303	0.7265	0.7269	7
Granodiorite, tonalite, qz diorite	0.7254-0.7329	0.7282	0.7264	3	0.7250-0.7323	0.7286	0.7286	2
Paragneiss and metavolcanic rock	0.7291-0.7396	0.7349	0.7361	3	0.7288-0.7325	0.7307	0.7307	2

stored at 4 °C until shipped for analysis. Prior to drying, plant leaves and berries were rinsed with MilliQ water. The plant and Pyhäjärvi fish flesh samples were dried at 70 °C for a minimum of 92 h prior to cryo-milling to powder.

In total, 79 human enamel or pars petrosa, 12 animal enamel, 9 human bones, 3 fish meat, 19 plants, and 17 water samples (139 samples in total) were collected for $^{87}Sr/^{86}Sr$ analysis. Correspondingly, a total of 78 human enamels and pars petrosas, and 15 animal enamel samples were selected for oxygen isotope analysis of bioapatite phosphate ($\delta^{18}O_p$).

In addition to the newly generated $^{87}Sr/^{86}Sr$ and $\delta^{18}O_p$ values, previously published data on the isotopic composition of carbon in the bioapatite carbonate ($\delta^{13}C_c$) and collagen ($\delta^{13}C_{coll}$), as well as collagen nitrogen isotope values ($\delta^{15}N_{coll}$) of the Luistari humans (Etu-Sihvola et al. 2022) are used and re-analysed to gain a more comprehensive understanding of people's mobility, their association to diet (food culture), the connections between use of food catchments and diet characteristics, and changes in them through time in the Luistari population. Out of the 79 samples analysed for $^{87}Sr/^{86}Sr$ values, 70 have a matching $\delta^{13}C_c$ value allowing for an extensive parallel evaluation of the three isotope systems (Table 1). The $\delta^{13}C_c$ values are used as a reflection of total diet, encompassing a signal from all macronutrient inputs, including carbohydrates and lipids not well represented in omnivore collagen $\delta^{13}C$ data (Krueger and Sullivan 1984; Lee-Thorp et al. 1989). Related to the general preservation pattern of organic tissue components at the cemetery, concentrated to the V II-III and V IV periods (Etu-Sihvola et al. 2022), a much more constrained number of data is available for collagen $\delta^{13}C$ and $\delta^{15}N$. Only 32 of the samples analysed for $^{87}Sr/^{86}Sr$ have matching values for the isotopic compositions of carbon and nitrogen of collagen, with the temporal distribution concentrated heavily to the V II-III ($n=14$) and V IV ($n=9$) periods, leaving the periods M I-II, V I and FP represented by only three, one and five samples, respectively. Thus, the entire dataset with a known period context assigned ($n=53$) presented by Etu-Sihvola et al. (2022) is used to evaluate the developments of dietary (protein) composition, with the period M I-II represented by six, V I by five, V II-III by 21, V IV by 14 and the FP by eight samples.

Methods

The strontium isotopic compositions of enamel, bone and environmental samples (water, plant leaves, fish meat) were determined at the Institute of Geology of the Czech Academy of Sciences. In case of enamel, the samples were subject to pre-treatment protocol that follows methods of Dudás et al. (2016). In brief, the protocol involves several leaching steps in MilliQ water-methanol (1:1) mixture followed by leaching in 0.1 M acetic acid buffered to pH of ~4.5 to remove possible clay and/or carbonate admixtures. Finally, the leached residues were washed several times in MilliQ water and dried. Afterwards, approximately 10 to 30 mg of the material was weighed and decomposed in the 2 ml of 14 M HNO3 for ~18 h on a hot plate at 110 °C. Subsequently, the resulted clear solution was dried down and re-dissolved in 2 ml of 1 M HNO3. The samples of plant leaves and fish meat were digested in a mixture of 5 ml ultrapure 14 M HNO3 with an addition of 200 µl of 24 M HF for ~16 h on a hot plate at 160 °C. Afterwards, the solutions were dried down and re-dissolved several times by a mixture of 14 HNO3 and 28% hydrogen peroxide to assure a complete decomposition and the final residue was collected in 1 M HNO3. Finally, about 10 ml of water sample was transferred to a 30 ml Savillex beakers and dried down. Subsequently, the residue was re-dissolved multiple times using a mixture of nitric acid-hydrogen peroxide, dried again and finally dissolved using 2 ml of 1 M HNO3. The strontium from all sample types was isolated by ion exchange chromatography using a Sr resin (Triskem). The samples were loaded in 1 ml of 1 M HNO3 whereas 2 ml of 0.05 M HNO3 was used for Sr collection (Pin et al. 2014). Strontium isotopic compositions ($^{87}Sr/^{86}Sr$) were determined using Thermo Triton Plus thermal ionization mass spectrometer (TIMS) using W filaments in the presence of Ta activator. During the course of this study, the periodical analyses of NIST 987 reference solution yielded $^{87}Sr/^{86}Sr$ of 0.710252 ± 0.000007 (2σ, $n=18$).

For the enamels, water, fish flesh and (diagenetic) bone samples, Sr concentrations were also determined by ICP-MS technique. For this purpose, remaining 1 ml of 1 M HNO3 solution was used for the analyses that was carried out by an Element 2 sector-field ICP-MS instrument hosted

at the Institute of Geology of the Czech Academy of Sciences using the methods outlined in Žák et al. (2016).

Diagenetic control was conducted through a correlation test, which involved assessing strontium concentrations against deviations of the $^{87}Sr/^{86}Sr$ ratios of human enamel from the $^{87}Sr/^{86}Sr$ composition of the burial environment (Reynard and Balter 2014; Martin et al. 2017). The latter is represented by the mean of the $^{87}Sr/^{86}Sr$ ratios measured in bones, as bones are particularly susceptible to diagenetic alteration (Bentley 2006; Montgomery 2010; Reynard and Balter 2014; Maurer et al. 2012; Lengfelder et al. 2019). This susceptibility is underscored by the marked general homogeneity of bone strontium values which is regularly observed. Detection of diagenetic alteration is possible when a mixing line appears between human and environmental values. The absence of this line in the case of Luistari (Supplementary Fig. 2) indicates that the samples were not subject to discernible diagenetic alteration.

For isotopic analysis of oxygen, Ag_3PO_4 was extracted according to the conventional precipitation procedure described in Sahlstedt and Arppe (2020) which represents an adaptation from the micro precipitation method of Wiedemann-Bidlack (2008). The Ag_3PO_4 crystals in tightly sealed high purity Ag capsules were loaded onto a Costech Noblank autosampler, and analysed at the Laboratory of Chronology of the Finnish Museum of Natural History on a Thermo Scientific EA Isolink setup with a pyrolysis temperature of 1450 °C. Oxygen yields (typically ca. 14%) were monitored and low O yield analyses, usually leading to lowered $\delta^{18}O_p$ values, were discarded. The $\delta^{18}O_p$ values were normalised using three Ag_3PO_4 materials: Nbs120c (21.7‰), AGPO-SCRI (14.58‰) and SJ-1 (in-house; 5.56‰), with the R^2 between expected and measured values > 0.99. Repeated measurements of the reference Ag_3PO_4 materials indicate an analytical precision within ± 0.4‰, while samples extracted in duplicate or triplicate were reproduced at ± 0.3‰ on average, however eight samples showed elevated SDs of 0.5–0.8‰ (Supplementary Table 1). The oxygen isotope composition of phosphate is reported in the delta (δ) notation as per mil (‰) deviations from the $^{18}O/^{16}O$ ratio of the VSMOW standard.

Data-analysis and statistical protocol

Data analysis and subsequent data visualisation were conducted using the R programming language within the integrated development environment RStudio. First, statistical tests were performed based on the normality of the data distribution and the number of variables within the study population. Both parametric and non-parametric tests were employed to ascertain statistical significance between variables. Initially, a normality test (Shapiro-Wilk test) was conducted on the dataset. This was complemented by visual aids such as QQ plots and histograms (Wickham 2016). Once the dataset was determined to exhibit a normal distribution, either a t-test (for comparisons involving two groups) or an ANOVA test (for comparisons involving three or more groups) was employed. For analyses involving data subsets and where the distribution was non-normal, non-parametric tests such as the Mann-Whitney test (for two groups) or the Kruskal-Wallis test (for three or more groups) were employed. The resulting p-value was subsequently assessed in conjunction with data visualisation (Greenland et al. 2016; Vaiglova et al. 2023). For statistical significance, the M I and M II periods were joined together.

The data obtained from environmental samples and both human and animal enamel were utilised to identify outliers and statistically evaluate the range of bioavailable strontium. Various statistical methods exist for outlier detection within a measured sample of a population, relying on the assessment of data dispersion. These methods include measures of scale such as standard deviation (SD), variance, interquartile range (IQR), or the median absolute deviation from the median (MAD), each differing in sensitivity to outliers (cf. Lightfoot and O´Connell 2016). These approaches are employed to describe the sample, establish boundaries, and subsequently calculate outliers by multiplying the measure of scale, such as 2SD or 3MAD (Lightfoot and O´Connell, 2016; Laffranchi et al. 2022; Scheeres et al. 2014; etc.). It is acknowledged that different methods have varying sensitivity to outlier identification, potentially resulting in false positives or false negatives (Lightfoot and O´Connell 2016; Szostek et al. 2015).

To overcome these issues, in this study the bioavailable strontium range and subsequent identification of human outliers were determined using Gaussian Kernel Density Estimate (KDE) applied to the entire dataset (including human enamel, animal enamel, water and plant samples), with data outliers removed using the calculation of the interquartile range as follows: 1.5 times the interquartile range was added to the third quartile and subtracted from the first quartile (Lightfoot and O´Connell 2016). This adjusted dataset was then utilised for the identification of Highest Density Intervals (HDIs) (Sheather and Jones 1991; Velte et al. 2023). The central tendency of the data was assessed using KDE with the assumption that KDE modes are relevant to the local population range. The RStudio hdrcde package was utilised to evaluate bioavailable strontium extent. Specifically, the hdr.den function was employed to compute and visualise HDIs, offering insights into bioavailable strontium distribution and different levels of certainty in the analysis. In this instance, HDIs were calculated at 90% and 99%, respectively (cf. Kruschke 2015), and are intended to define the bioavailable strontium range of the Luistari population.

Various spans of the data distribution represent the degree of encompassing possible variation, with 90% being the most benevolent for the outlier identification and 99% being the most conservative.

Using these methods, non-local individuals were identified as those whose values statistically deviated from the defined bioavailable $^{87}Sr/^{86}Sr$ range. Subsequently, these individuals were compared with the remaining isotopic evidence, including bioapatite $\delta^{18}O_p$ and $\delta^{13}C_c$, as well as dental collagen $\delta^{13}C_{coll}$ and $\delta^{15}N_{coll}$ values previously analysed by Etu-Sihvola et al. (2022). This comparison with additional evidence aims to strengthen the statistical significance of outliers by assuming that non-local individuals should exhibit different childhood diets in addition to diverse food catchments represented by $^{87}Sr/^{86}Sr$ ratios and $\delta^{18}O_p$ values. It is expected that by incorporating other isotopic evidence alongside archaeological contextualisation, non-local individuals not detected by statistical methods alone could also be identified.

For $\delta^{18}O_p$, $\delta^{13}C_c$, $\delta^{13}C_{coll}$ and $\delta^{15}N_{coll}$ simple statistical evaluations of normality (Shapiro Wilk test), outlier detection (Grubb's test), and testing for differences among group central values and distributions (Kruskal Wallis test, Dunn's test) were computed using Origin 2024 software.

In addition to identifying non-local individuals, the variability within the skeletal $^{87}Sr/^{86}Sr$ datasets divided according to chronological periods (see *Materials* for period definitions) was also considered as a significant indicator of the characteristics of the Luistari population and the potential identification of the use of different food catchments across different chronological phases. The underlying assumption is that if the local community shares broadly similar dietary habits and exploits the same food catchment area, its isotopic values should exhibit homogeneity, as opposed to more dispersed values observed when the community exploits different food catchments or has varied dietary habits caused, among others, by different childhood diets. To assess the measure of variability within individual chronological phases, Euclidean Distances (ED) from the means for individual variables (i.e. the isotopic values) were calculated. The advantage of this approach lies in its multidimensional nature, i.e. in the possibility of involving more than one variable in the equation (Beaver and Dean 2019). In this instance, the $^{87}Sr/^{86}Sr$ ratios were combined with the bioapatite $\delta^{13}C_c$ values to encompass both the geological background and dietary variations. The choice of included isotope values was additionally guided by obtaining the maximum number of independent observations, as the $^{87}Sr/^{86}Sr$ and $\delta^{13}C_c$ values were available for the entire dataset unlike the $\delta^{13}C_{coll}$ and $\delta^{15}N_{coll}$ values.

The EDs were calculated as $ED(x, x0) = \sqrt{\sum_{i=1}^{n} (x_i - x0_i)^2}$ where x represents variables, and $x0$ represent the variable means. The resulting EDs were then compared using Gaussian KDEs.

Results

Environmental baseline

The $^{87}Sr/^{86}Sr$ values of the water, plant and fish samples display a considerable range from 0.7204 to 0.7734 (Supplementary Table 2). The highest value is an outlier (Grubb's test, $p=0.0008$), obtained on birch (*Betula pendula*) leaves from the western Rapakivi granite area. The overall mean $^{87}Sr/^{86}Sr$ values for all water and plant samples are 0.7294 ± 0.0048 and 0.7353 ± 0.0113, respectively (Figs. 3 and 4:A).

The samples of pike, roach and perch flesh caught from lake Pyhäjärvi cluster at 0.7296 ± 0.0002, while the water samples ($n=3$) collected from both the northern and southern reaches of the lake show rather uniform values at 0.7302 ± 0.0001. Thus, aquatic dietary contributions from lake Pyhäjärvi are expected to have $^{87}Sr/^{86}Sr$ values around 0.730 (Fig. 4:A, dark blue symbols). The two major inlet rivers with catchments to the south and east of the lake showed mutually similar $^{87}Sr/^{86}Sr$ levels at 0.7323 and 0.7325, somewhat higher than the Sr isotope value of the lake itself. The lower lake $^{87}Sr/^{86}Sr$ value might reflect the influence of the Satakunta sandstone underlying the lake. This would be consistent with observations from regional groundwaters, where aquifer units affected by dissolution of calcite with presumed low $^{87}Sr/^{86}Sr$ derived from the sandstone yield low $^{87}Sr/^{86}Sr$ values (0.718–0.719) compared to unaffected units (0.736–0.751; Kortelainen and Karhu 2009).

To evaluate differences among bedrock areas, the plant and water samples were assigned to one of the four major rock types common in the surveyed area (Supplementary Table 2). For rivers and streams, rock type was assigned based on sampling coordinates. For lakes, the assignment was made according to the majority of area covered by the lake. The ranges of $^{87}Sr/^{86}Sr$ values among the rock types show overlap and differences in distributions are not statistically significant (Kruskal-Wallis test, $p=0.28$), but there is a tendency for both water and plant samples collected on the Rapakivi granite area to show highest $^{87}Sr/^{86}Sr$ values, followed by those on the southern metamorphic rocks (Table 2). This is in agreement with the mineralogy of these units containing high proportions of minerals with high Rb/Sr ratios (mica, K-feldspar) and therefore, largely radiogenic $^{87}Sr/^{86}Sr$ values. Thus, tendencies to higher $^{87}Sr/^{86}Sr$ values are observed more commonly to the west and south/southeast of lake Pyhäjärvi, where also the thickness of surficial

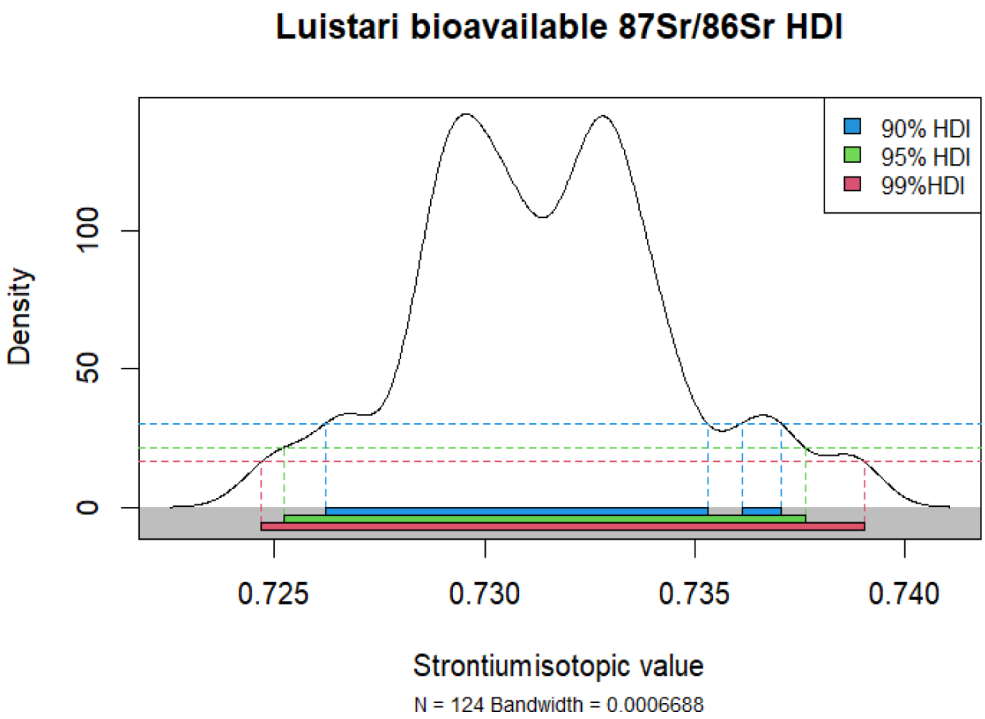

Fig. 3 Kernel Density Plot of the whole dataset with HDI intervals for 90%, 95% and 99%, respectively. KDE is calculated based on Gaussian Kernel using R package hdrcde and ggplot2 (Wickham 2016) for visualisation

sediments is the thinnest (see Geographical and geological background above).

The nine samples of archaeological human bone yielded a mean $^{87}Sr/^{86}Sr$ value at 0.7326 ± 0.0013 for the diagenetic environment, a value close to the mean/median values of water samples collected from the Rapakivi granite area on which the Luistari cemetery is situated (Table 2). On the other hand, a much lower value of 0.7225 was obtained on leaves of a birch growing at the cemetery. This, as well as the larger scatter of the plant sample data, illustrates the more spot-like nature of plants as proxies for bioavailable $^{87}Sr/^{86}Sr$ values compared to rivers, lakes and streams reflecting a more averaged signal of the catchment area (Bentley 2006; Maurer et al. 2012).

To explore local geospatial patterns, the $^{87}Sr/^{86}Sr$ values of the water and plant samples were projected onto a geological map of the surveyed region (Supplementary Fig. 3). For sampling sites where both water and plants were collected, and where both sample types are underlain by the same rock type (e.g. not the case for lake Pyhäjärvi water and plants collected from its western Rapakivi shores), a mean $^{87}Sr/^{86}Sr$ value was calculated for plotting (Supplementary Table 2). The distribution of values suggests an area of lower $^{87}Sr/^{86}Sr$ values, typically < 0.730, in the area north/northeast of lake Pyhäjärvi, while values > 0.732 are more common for the western, southern and southeastern sectors.

The Sr concentrations of the water samples varied from 12 to 114 ppb (Supplementary Table 2), similar to values of rivers and other surface waters in Finland and Sweden (Löfvendahl et al. 1990; Blank et al. 2018). Lake Pyhäjärvi showed an average Sr concentration of 35 ± 0.8 ppb ($n = 3$). Pyhäjärvi fish flesh had Sr concentrations at 1–3 ppm, in line with values presented for Finnish pike and perch by Varo (1982).

Strontium isotope compositions ($^{87}Sr/^{86}Sr$)

Human $^{87}Sr/^{86}Sr$ values range from 0.7245 to 0.7432 with a mean value at 0.7318 (SD 0.0032, $n = 79$) (cf. Table 3). The normality of the assemblage was tested using Shapiro-Wilk test and confirmed at $p = 0.00004$. The bioavailable range estimated using KDE analysis of the whole assemblage yielded ranges of 0.7262 to 0.7353 at 90% and 0.7246 to 0.7390 at 99% of the highest density intervals (Fig. 3). The majority of the human samples are within the estimated bioavailable range, suggesting that most sampled individuals spent their childhood or adolescent years in the area. There is a visible separation into two groups of samples around the $^{87}Sr/^{86}Sr$ values of 0.732–0.733 (Fig. 4:A) which is reflected also in the bimodality of the KDE plot (Fig. 3).

Individual chronological phases display comparable $^{87}Sr/^{86}Sr$ ranges similar to the estimated bioavailable local range, however, there are differences within their minimum and maximum values (Table 3). Differences in strontium isotope ratios among individual chronological phases were evaluated statistically without an indication of marked differences between the main ranges of the data (Kruskal-Wallis test, $p = 0.0964$). Visually, however, the differences

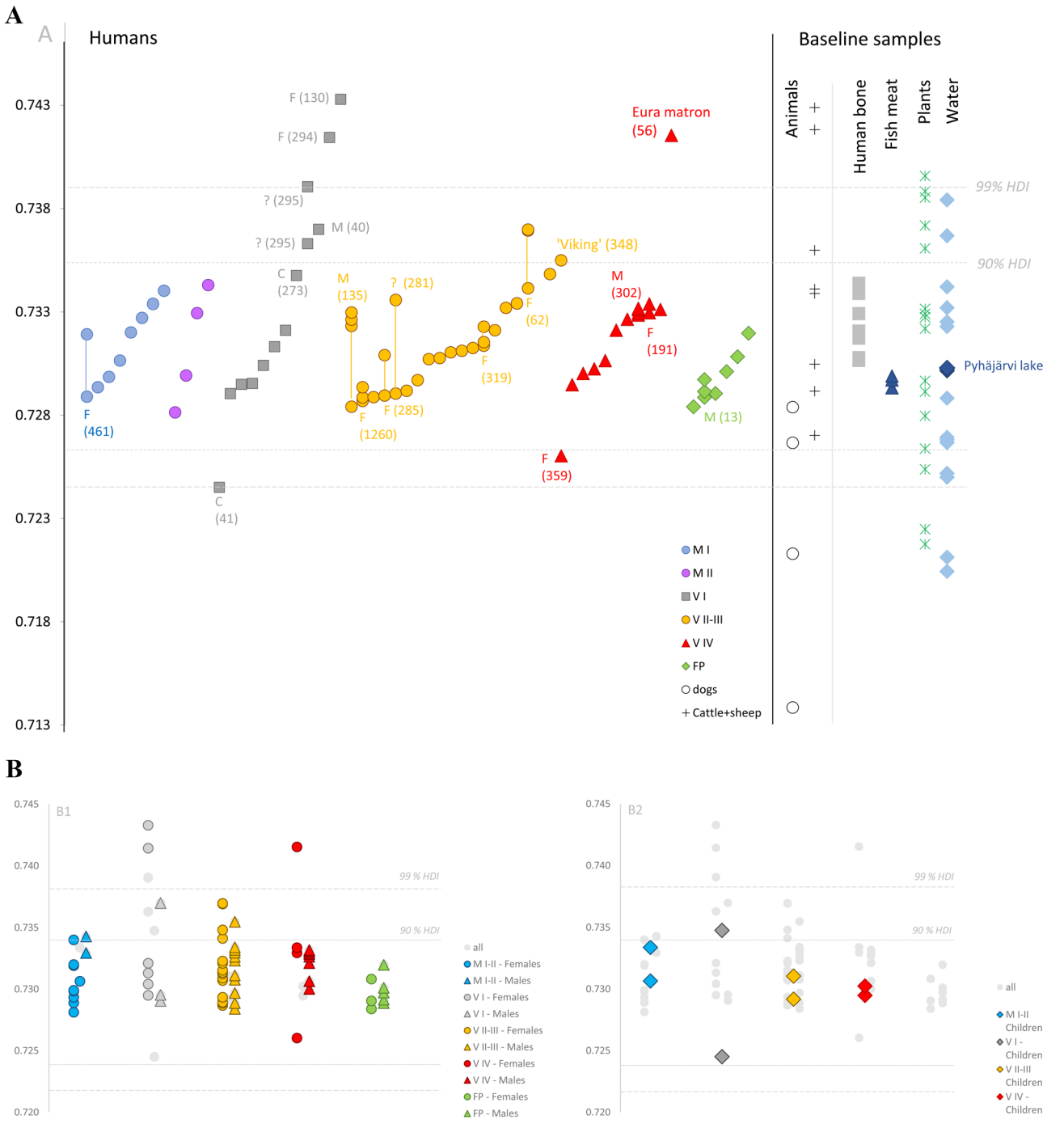

Fig. 4 $^{87}Sr/^{86}Sr$ ratios of analysed samples categorised according to chronological phases of the cemetery (**A**), and sex and age categories (**B**1,2). Horizontal lines indicate ranges of bioavailable strontium estimated from the statistical analysis (90% and 99% HDIs) of the human and environmental samples (animal enamel, plants, waters). Outliers and multiply sampled individuals are indicated by grave numbers and biological sex if available (**A**). Multiple samples from one individual are connected with vertical lines (**A**). One plant sample with $^{87}Sr/^{86}Sr$ at 0.77337 is outside the range covered by the vertical axis. Analytical errors are smaller than the symbol size

Table 3 Summary of the descriptive statistical values for the whole dataset (supplementary table 1) of the human and animal values from the Luistari cemetery. $\delta^{13}C_c$ data are after etu-Sihvola et al. 2022

	$^{87}Sr/^{86}Sr$					$\delta^{13}C_c$					$\delta^{18}O_p$				
	mean	median	range	SD	*n*	mean	median	range	SD	*n*	mean	median	range	SD	*n*
HUMANS-WHOLE DATASET	0.7319	0.7314	0.7245-0.7433	0.0032	*79*	-14.5	-14.6	-15.9- -12.4	0.6	*70*	15.8	15.9	13.4-18.4	1	*78*
M I+II	0.7314	0.7319	0.7281-0.7343	0.002	*13*	-15.1	-15.1	-15.5- -14.8	0.3	*12*	15.9	15.7	14-17.2	0.9	*10*
V I	0.7337	0.7321	0.7245-0.7433	0.0055	*13*	-14.7	-14.9	-15.9- -12.7	0.8	*13*	15.6	15.8	14.1-16.7	0.7	*11*
V II+III	0.7317	0.7313	0.7284-0.7370	0.0024	*30*	-14.3	-14.3	-15.1- -13.2	0.5	*30*	15.7	15.9	13.4-18.4	1.2	*27*
V IV	0.7323	0.7329	0.7260-0.7415	0.0033	*15*	-14.4	-14.6	-15.7- -12.3	0.7	*15*	16	16.5	13.4-17	1.1	*15*
FP	0.7298	0.7294	0.7284-0.7320	0.0012	*8*	-14.5	-14.5	-15.3- -13.8	0.5	*8*	16.2	16.4	15-17.3	0.9	*7*
cattle, sheep	0.7319	0.7340	0.7270-0.7429	0.0052	*8*	-12.7	-12.4	-15.4- -10.6	1.5	*10*	13.6	13.5	11.2-15.5	1.5	*9*

between the data distribution within the individual kernel ranges are apparent (Supplementary Fig. 4).

Further, no statistically significant differences were observed between males and females (Mann-Whitney test, $p=0.3729$). When considering the temporal aspect, it is important to note that not all periods yield a sufficient number of samples for statistical analysis. Visual comparison (Fig. 4:B1) primarily reflects the uneven proportions of male and female graves available for sampling across individual periods. Despite these limitations, certain patterns of sex-dependent mobility can be inferred. While periods V I and V IV show larger offsets of the outliers, specifically in case of females, there are no discernible differences in mobility patterns between males and females in the remaining periods, regardless of the magnitude of the outlier offset.

In the case of children, there is a general observation that they serve as good proxies for determining local bioavailable ranges, based on the assumption that their short lives limit opportunities for relocation (Knipper et al. 2020). All sampled children in the Luistari cemetery align with this observation, with the exception of period V I. In this period, both child graves returned outlying $^{87}Sr/^{86}Sr$ values; one beyond the 90% range (0.7347, grave 273), and one beyond the 99% range (0.7245, grave 41). Both child graves are also visibly offset from the rest of the group (Fig. 4:B2).

$^{87}Sr/^{86}Sr$ values of twelve archaeological faunal enamel samples range from 0.7138 to 0.7428 with an average of 0.7304 (SD 0.0081, $n=12$). Out of eight samples for cows and sheep two samples are outside the 99% HDI range and one is outside the 90% HDI range. One of these, a cow sample from grave 1008, is from a late burial not contemporaneous with the rest of the graves. As the highly radiogenic animal samples lack comparative values in the bio-available strontium dataset, their non-local origin can be assumed. The 99% HDI outliers have similar $^{87}Sr/^{86}Sr$ values as the outlying human enamels. Similarly to human samples, there is also a visible gap between two groups of samples around the $^{87}Sr/^{86}Sr$ value of 0.732. Conspicuously different values were observed for dogs (Fig. 4:A) with the lowest $^{87}Sr/^{86}Sr$ value being as low as 0.7138 (grave 480), and the second lowest is 0.7212 (grave 289).

Oxygen isotopes ($\delta^{18}O_p$)

The $\delta^{18}O$ values of bioapatite phosphate were obtained for altogether 78 human samples, and yielded a total range of 5‰, from 13.4 to 18.4‰. The full dataset is drawn from a normal distribution (Shapiro-Wilk test, $p=0.47$) and has a mean value of 15.8 ± 1.0‰ (Table 3). Overall, the $\delta^{18}O_p$ values show a dispersed, but continuous distribution without statistical outliers (Grubb's test, $p=0.84$, $n=78$). The dispersion is very similar to the average range (5.1–5.2‰)

reported for sites with sample $n>40$ in an overview of site ranges in archaeological $\delta^{18}O_p$ data globally (Lightfoot and O'Connell 2016). The variation is linked to variability in environmental waters further modified by human behaviour (diet composition, cooking methods, use of non-local foods) and physiological differences (Daux et al. 2008; Lightfoot and O'Connell 2016). For the Luistari population, drinking water likely came from variable sources with expected differences in $\delta^{18}O_w$ values. For example, waters of both the extensive Pyhäjärvi lake and its outlet river Eurajoki were likely to show $\delta^{18}O_w$ values higher than those of precipitation due to evaporative effects in lakes with large surface areas, while springs and groundwater fed streams related to the glaciofluvial formations in the east would show lower $\delta^{18}O_w$ values closer to longer term averages of $\delta^{18}O_w$ in mean annual precipitation.

As a consequence of the continuously dispersed distribution of the $\delta^{18}O_p$ values, samples with outlier values for $^{87}Sr/^{86}Sr$ did not present $\delta^{18}O_p$ values conspicuously apart from the main distribution of the full dataset (Fig. 5; Supplementary Fig. 5). However, within period specific datasets, the $^{87}Sr/^{86}Sr$ outliers from graves 56 and 359 were observed to show the lowest (gr. 56) and highest (gr. 359) $\delta^{18}O_p$ values of period V IV. At the same time, all $^{87}Sr/^{86}Sr$ outliers of period V I were well within the typical $\delta^{18}O_p$ values for the period, similar to the period and full dataset means at 15.6±0.7‰ and 15.8±1.0‰, respectively.

The highest variance, along with the highest and lowest $\delta^{18}O_p$ values for the entire dataset, were observed for the V II-III period in contrast to the $^{87}Sr/^{86}Sr$ value range peaking at period V I. Instead of reflecting changed patterns of e.g. increased differences in drinking water sources or the makeup and preparation of food, all relevant to human $\delta^{18}O_p$ values, this is considered a reflection of the higher number of samples analysed for V II-III ($n=30$) compared to the other periods ($n=8$–15) (Lightfoot and O'Connell 2016).

The period specific distributions (Table 3; Supplementary Fig. 5) suggest a generally increasing trend from period V I to FP, but differences are not statistically significant (Kruskal Wallis test, $p=0.58$). However, when considered together with the temporal increases in $\delta^{13}C_c$, $\delta^{13}C_{coll}$ and $\delta^{15}N_{coll}$ values (see below, Supplementary Fig. 5), the tentative increasing trend in $\delta^{18}O_p$ values might be linked with increasing temperatures, consistent with the amelioration of climate from the 'Dark Ages Cold Period' to the 'Medieval Warm period' (e.g. Mann 2009; Helama et al. 2017; Ljungqvist 2010). Samples assigned to males and females showed overlapping ranges with similar central tendencies to the overall dataset, with female $\delta^{18}O_p$ showing a larger overall range.

The $\delta^{18}O_p$ values of animals buried at Luistari yielded lower $\delta^{18}O_p$ values than humans. Cattle ($n=5$, mean 13.5‰, SD 1.4, median 13.1‰) and sheep ($n=5$, mean 13.1‰, SD 1.5, median 13.4‰) gave mutually similar values for a combined domestic herbivore mean at 13.3±1.36‰. The $\delta^{18}O_p$ values of dogs ($n=4$, mean 14.0‰, SD 0.9, median 14.2) were similar to those of the herbivores (t-test, $p=0.33$). A single $\delta^{18}O_p$ value obtained from an undated pig enamel at 16.3‰ was closer to the mean value of humans than those of the other animals. The lower animal $\delta^{18}O_p$ values are interpreted to primarily reflect taxon specific differences in physiology and oxygen fractionation (e.g. Luz et al. 1984; Bryant and Froelich 1995) as well as differences in source of ingested water ('raw' vs. processed waters for animals vs. humans).

Carbonate carbon isotopes ($\delta^{13}C_c$)

After rejection of a single high outlier value at -12.3‰ from the period FP, the $\delta^{13}C_c$ dataset shows a normal distribution (Shapiro-Wilk test, $p=0.54$) with a mean at -14.5‰ (SD 0.6, $n=69$) (Table 3). When categorised according to

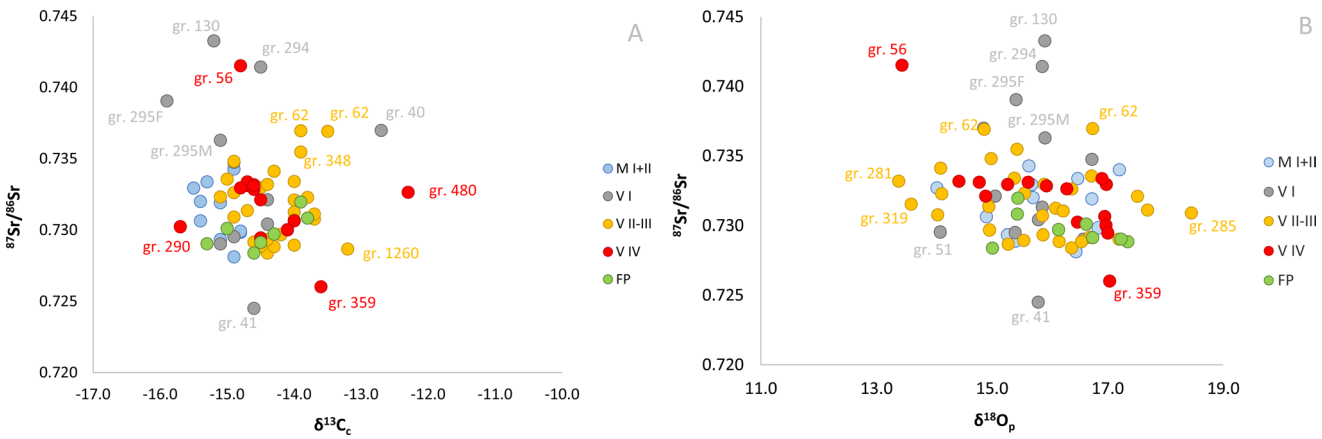

Fig. 5 Scatterplot of the $^{87}Sr/^{86}Sr$ and $\delta^{13}C_c$ (**A**), and $^{87}Sr/^{86}Sr$ and $\delta^{18}O_p$ (**B**) with symbols color coded according to individual chronological periods. Individuals distinct from and on the fringes of the main period specific distributions are marked by grave numbers

periods, the $\delta^{13}C_c$ distributions show significant differences (Kruskal Wallis test, $p=0.0003$) and suggest a temporally increasing trend (Supplementary Fig. 5). While the $\delta^{13}C_c$ values for the M I-II and V I periods are not statistically different, nor are the mutual mean values of the ensuing V II-III to FP $\delta^{13}C_c$ data, the $\delta^{13}C_c$ values of combined M I-II and V I periods (median −14.7‰, $n=21$) are significantly lower (Mann-Whitney test, $p<0.0001$) than those of the combined V II-III to FP samples (median −14.0‰, $n=49$). Thus, the reduced dataset used here replicates the findings of a temporal increase in human enamel $\delta^{13}C_c$ values originally reported by Etu-Sihvola et al. (2022).

Collagen carbon and nitrogen isotopes ($\delta^{13}C_{coll}$, $\delta^{15}N_{coll}$)

Excluding the single deciduous tooth (KM 26695:18; gr 1061) with a distinctively high $\delta^{15}N_{coll}$ value at 16.6‰ suggesting traces of breastfeeding (e.g. Tsutaya and Yoneda 2015), the $\delta^{13}C_{coll}$ and $\delta^{15}N_{coll}$ values show normal distributions (Shapiro Wilk test, $\delta^{13}C_{coll}$ $p=0.99$, $\delta^{15}N_{coll}$ $p=0.31$, $n=52$) with means at -20.1 ± 0.5‰ and 13.1 ± 0.8‰, respectively. For a Finnish inland population, the $\delta^{13}C_{coll}$ values are relatively high, often comparable to those of more coastal or island context archaeological populations. This feature is interpreted not to primarily reflect systematic marine (brackish) dietary input, but is linked with the influence of the calcite bearing Satakunta sandstone formation underlying the Pyhäjärvi lake and much of the northern Eurajoki river lands (Etu-Sihvola et al. 2022). The $\delta^{15}N_{coll}$ values at the population level are high, indicating systematic substantial reliance of animal protein from higher trophic levels, and interpreted to reflect the influence of aquatic resources from the fish-rich Pyhäjärvi lake, as well as the rivers and smaller lakes in the region (Etu-Sihvola et al. 2022). At the same time, the $\delta^{15}N_{coll}$ distribution shows considerable variance, with lowest values at 11–12‰ (e.g., graves 56, 62, 281, 480), indicating significant dietary variability among the individuals buried in Luistari.

In line with observations for $\delta^{13}C_c$, there are also significant differences in $\delta^{13}C_{coll}$ values among the different periods (Kruskall-Wallis test, $p=0.0002$; Supplementary Fig. 5). The values of the M I-II and V I periods are statistically the same, but significantly lower than the $\delta^{13}C_{coll}$ values for the V II-III period (Dunn's Test, M I-II $p=0.01$, V I $p=0.049$). Further, the V II-III period shows significantly higher $\delta^{13}C_{coll}$ values than the subsequent V IV period ($p=0.009$). Similarly, there is a statistically significant difference in period-specific $\delta^{15}N_{coll}$ values (Kruskal Wallis test, $p=0.02$), yet the individual paired comparisons (Dunn's test) only discover a significance at 90% level for the $\delta^{15}N_{coll}$ values between periods V I and V IV ($p=0.07$), possibly due to the low number of data for periods M I-II and V I and the larger variance compared to $\delta^{13}C_{coll}$ values. When the mutually similar periods M I-II and V I are pooled ($n=10$), the combined M I-II to V I $\delta^{15}N_{coll}$ values are significantly lower than those of period V IV (Dunn's test, $p=0.008$) that are statistically indistinguishable from periods V II-III and FP.

Outliers and their characteristics

Several potentially non-local individuals were identified based on their outlying $^{87}Sr/^{86}Sr$ values. Out of a total of 79 individuals, four were outside of the upper 99% HDI range of the bioavailable strontium (graves 56, 130, 294, 295; see Fig. 4:A and Fig. 5). Their values exhibit higher radiogenic nature, clustering around the value of 0.740. Additionally, several other graves (graves 273, 62, 40) were identified as more radiogenic strontium outliers based on their position outside the 90% of the HDI range of the bioavailable strontium. Two of the graves (41, 359) display notably less radiogenic $^{87}Sr/^{86}Sr$ ratios, around the value of 0.725 (grave 41 was outside 99% range, grave 359 was outside 90% range).

The chronological dynamics of the outliers can be presented as follows (Fig. 4:A, Supplementary Fig. 4): during the Merovingian period, there are no outliers detected within 99 nor 90% bioavailable HDI ranges. However, in the subsequent V I period, there is an increase in numbers of burials and also a notable increase in the number of outliers observed outside the 99% HDI range, totaling four individuals (graves 41, 130, 294, 295). Additionally, two further outliers are identifiable based on the 90% HDI range (graves 40, 295). Notably, the child in grave 273 also exhibits a deviation from the main cluster of strontium values, although statistically, the value remains within the 90% bioavailable range. In the V II-III period, statistical outliers are exclusively found outside the 90% HDI range (graves 348 and 62). Conversely, during the V IV period, individuals with distinct outlying values are observed in contrast to the well-defined homogeneous core values. One grave falls outside the 99% range (grave 56), while another is identified outside the 90% range (grave 359). Similarly to the earliest period, the latest period (FP) does not present any outliers beyond the local bioavailable range.

When integrating the Sr isotope values with other isotopic evidence and archaeological context, the individuals statistically identified as non-local based on their outlying $^{87}Sr/^{86}Sr$ values can also be distinguished by their distinct dietary isotopes (such as the case of the graves 56, 62, 294 or 359) (Supplementary Table 1). Different dietary patterns are primarily characterised by less negative $\delta^{13}C$ values (both collagen and carbonate) and either lower or higher $\delta^{15}N_{coll}$ values compared to the typical values of the population.

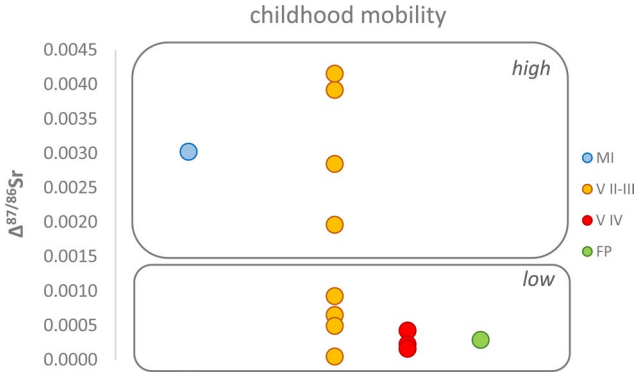

Fig. 6 Childhood mobility patterns in Luistari in different chronological phases. The threshold value of 0.001 is used here graphically as a conventional separator between more or less pronounced childhood mobility. For sample numbers and exact values see Supplementary Table 3

Furthermore, in several cases, such individuals are discernible by specific grave goods or costume parts (Supplementary Table 1).

Some other potential non-locals, in terms of individuals with light stable isotope values at the fringes of the main cluster albeit not anomalous by their $^{87}Sr/^{86}Sr$ ratios, can be highlighted, particularly based on $\delta^{13}C_c$ values (graves 290, 480, 1260), but also $\delta^{18}O_p$ values (graves 51, 281, 285, 319) (Fig. 5), especially when considered within the distributions of individual periods.

Chronological variations in mobility patterns were furthermore observed among multiply sampled individuals (Supplementary Table 3, Fig. 6). As the $\Delta^{87}Sr/^{86}Sr$ offset of 0.001 between sampled molars or premolars is conventionally regarded as a threshold value for childhood relocation (Knipper et al. 2018; Hrnčíř and Lafoon 2019), contingent upon the overall environmental conditions and numerous other factors, it was similarly employed here as a potential dividing line between more or less pronounced mobility behaviour in terms of distance. Although the varying number of sampled individuals across chronological periods presents a challenge for a robust comparison, it is evident that the offsets between different sampled tissues (primarily between M1, M2/PM, and M3) are more pronounced in the early chronological phase (M I). While the most represented period (V II-III) exhibits varied ranges of childhood mobility behaviour, the later phases display minimal differences between sampled teeth.

ED characteristics

In terms of the data patterns (Table 4, Supplementary Fig. 6) reported by calculating the Euclidean distances, the two earliest periods (M I+II and V I) exhibit similar, slightly less homogeneous pattern than the two following periods,

Table 4 Euclidean distances from the mean statistics calculated jointly for the $^{87}Sr/^{86}Sr$ and $\delta^{13}C_c$ for the individual chronological phases

Period	*n*	mean	max	min	SD
M I+II	10	0.3200	0.0017	0.0200	0.2290
V I	11	0.5273	2.0000	0.1004	0.5711
V II-III	27	0.3981	1.0519	0.0482	0.2652
V IV	14	0.5143	2.1000	0.0800	0.5545
FP	7	0.4163	0.8143	0.0143	0.3096

which could be attributed to a comparatively lower sample count. The most homogeneous groups according to the ED within the $^{87}Sr/^{86}Sr$ and $\delta^{13}C_c$ clusters, are periods V II-III and V IV, although with noticeable outliers (Supplementary Fig. 6). The final period displays a higher variability in $\delta^{13}C_c$, despite having more centred $^{87}Sr/^{86}Sr$ values, indicating lower degree of homogeneity. Nonetheless, it is important to note that this group may be the most influenced by the lower sample count bias.

Food catchments

The bimodal distribution of the Gaussian KDE (Fig. 3) clearly indicates that within the entire assemblage, there are two groups - one with less radiogenic and the other with more radiogenic $^{87}Sr/^{86}Sr$ values, delineated roughly around the value of 0.732/0.733 (Figs. 3 and 4). This pattern is visible for both human and the animal samples. The distinctive gap between the two ranges of strontium values may suggest the existence of two geographically constrained food catchment zones, a hypothesis reinforced by the geographical distribution of the environmental samples (Fig. 7). Areas with lower $^{87}Sr/^{86}Sr$ values, typically <0.730 are observed to the north and northeast of lake Pyhäjärvi, underlain by sandstone and eastern felsic rocks, whereas higher values >0.732 are common in the western Rapakivi granite areas and southern/southeastern metamorphic rock areas.

These designated food catchment zones, labelled as Zone 1 (north of Pyhäjärvi lake) and Zone 2 (in the wider surrounding area), demonstrate significant disparities also in the dietary isotopes of the Luistari burial community, both as a whole and throughout its chronological development.

Figure 8 shows the $\delta^{13}C_{coll}$ and $\delta^{15}N_{coll}$ values of samples assigned to Zone 1 and Zone 2, respectively (Supplementary Table 1). Disparities between the two distinct food catchments are especially observed in the case of $\delta^{13}C_{coll}$ values (Mann-Whitney U test, $p=0.001088$, $n=46$), but less so in the case of $\delta^{15}N_{coll}$ (Mann-Whitney U test, $p=0.639648$, $n=46$). Visually, the contrast in $\delta^{13}C_{coll}$ values between the two zones is evident (Fig. 8), with more positive $\delta^{13}C_{coll}$ in Zone 1. Additionally, the $\delta^{15}N_{coll}$ values in Zone 1 appear more tightly clustered than those in Zone 2. Upon comparing the isotope values from different time periods within each food catchment both graphically and statistically (those

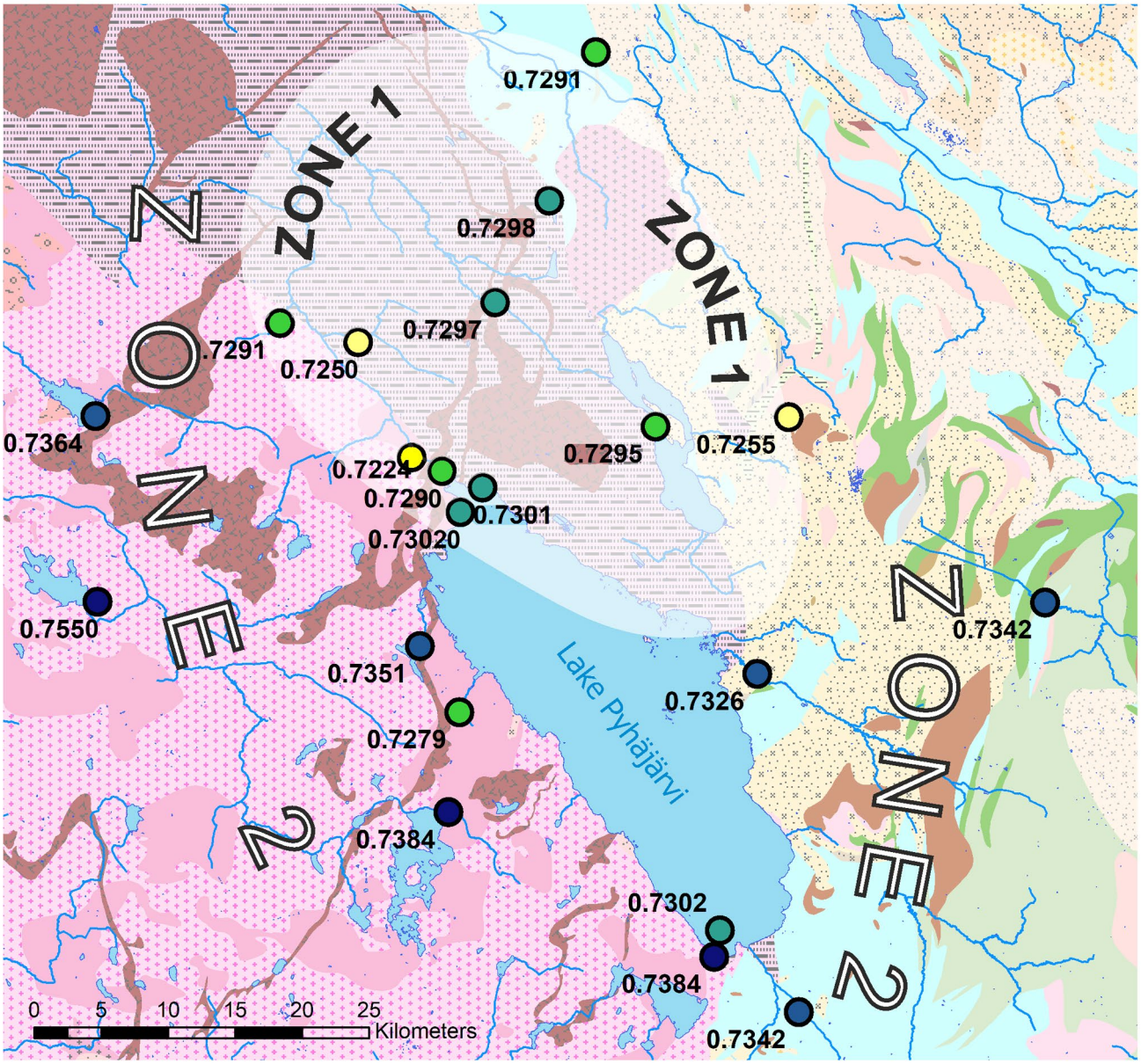

Fig. 7 Two possible hinterland zones (Zone 1 and 2; see text "Food catchments") based on the different $^{87}Sr/^{86}Sr$ ratios of the environmental samples (for the legend on the geological units see Supplementary Information 2). Data sources: Bedrock of Finland 1:200 000 from the Geological Survey of Finland GTK. River network dataset from the Finnish Environment institute SYKE

with minimum number of samples = 5), it becomes apparent that stable isotopic values are more uniform in Zone 1 (Kruskal-Wallis, $\delta^{13}C_{coll}$, $p = 0.2724$; $\delta^{15}N_{coll}$, $p = 0.1708$), whereas in Zone 2, the chronological periods are distinctly separated (Kruskal-Wallis, $\delta^{13}C_{coll}$, $p = 0.0112$; $\delta^{15}N_{coll}$, $p = 0.0225$) (Fig. 9).

The clustering of $\delta^{13}C_{coll}$ values in Zone 1, especially in the V II-III period, is apparent. This, complemented by a homogeneity of $\delta^{15}N_{coll}$ values over time, suggests relatively unchanged dietary patterns. The overall consistency of dietary isotopes in this zone may indicate resource exploitation which was stable over time, portraying it as a "subsistence-traditional" zone. Conversely, in Zone 2, samples show much more variation in $\delta^{15}N_{coll}$, suggesting a more diverse nature of dietary inputs. Additionally, the $\delta^{13}C_{coll}$ values in this zone are generally more negative. Furthermore, the differences across the periods allow for the temporal aspects of the subsistence economy to be considered as well. Zone 2 can be thus interpreted as more "subsistence-opportunistic" and individualistic, reflecting the local environment or climate, and diverse patterns of land exploitation. These disparities in landscape exploitation

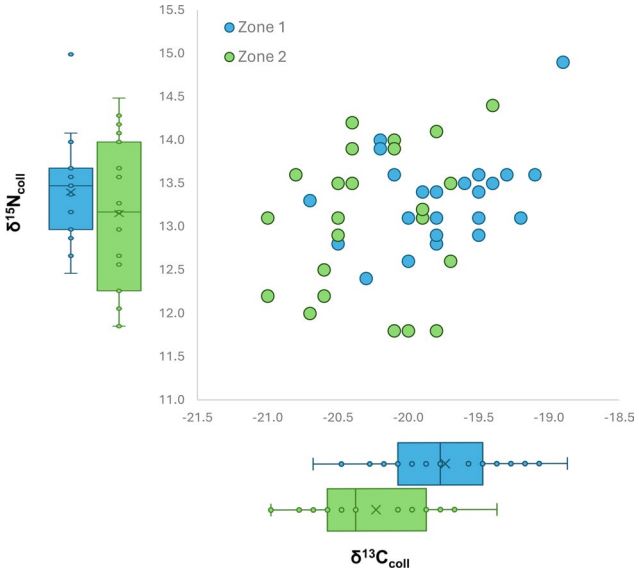

Fig. 8 Comparison of the dietary isotopes within the two food catchment zones predicted by $^{87}Sr/^{86}Sr$ ratios. The difference in $\delta^{13}C_{coll}$ values is statistically significant

between the two zones are noticeable not only across different periods but also within a single phase. During period V II-III, a substantial contrast emerges, with Zone 1 showcasing clustered and less negative $\delta^{13}C_{coll}$ values alongside higher $\delta^{15}N_{coll}$ values. In contrast, Zone 2 displays more scattered values, lower $\delta^{15}N_{coll}$, and more negative $\delta^{13}C_{coll}$. This suggests a diversification in the subsistence economy in response to diverse environmental conditions, and potentially distinct settlement patterns as well.

It is worth noting that significantly lower $\delta^{15}N_{coll}$ values, previously linked to individuals of elite status (Etu-Sihvola et al. 2022), were predominantly confined to Zone 2, i.e., to areas with more radiogenic strontium background. Since the nitrogen values in Zone 2 do not reveal any discernible trends indicative of environmental or subsistence patterns, the presence of notably low nitrogen values among the chosen individuals may potentially be linked to the residences of elite members of the society.

Discussion

Drawing upon the presented multi-isotopic evidence and archaeological contextualisation, we can delineate the population and settlement dynamics and its temporal evolution.

Merovingian period (M I - M II, 550–800 CE)

In the early Merovingian period (M I), graves were dug in rows, but during the later Merovingian period (M II), the orientation started to shift (Lehtosalo-Hilander 1982b: 177). Based on the preserved graves, M I is mostly dominated by female graves, and M II by male graves, while children's graves appear in the cemetery during both periods (Lehtosalo-Hilander 2000: 227). During the earliest Merovingian period (550–750 CE), the isotopic data suggest a relatively stable local community. Despite the limited data available compared to the two centuries time span they represent, the datasets appear fairly uniform in the dual Sr-C and Sr-O isotopic spaces (Fig. 5), albeit according to ED with slightly larger spacings between points compared to other periods (Fig. 5, Supplementary Fig. 6). In terms of subsistence, the higher EDs might indicate less group-consistent exploitation of the landscape. The range of $^{87}Sr/^{86}Sr$ values (Fig. 4:A) also suggests the utilisation of a broader environmental catchment around Eura, encompassing all the major bedrock types in the surroundings of lake Pyhäjärvi thus establishing a wider catchment area for communities in subsequent phases. Both the $^{87}Sr/^{86}Sr$ ratios and the patterning of $^{87}Sr/^{86}Sr$ and $\delta^{13}C_c$ data may indicate a loosely structured settlement, possibly consisting of individual farms or smaller settlements.

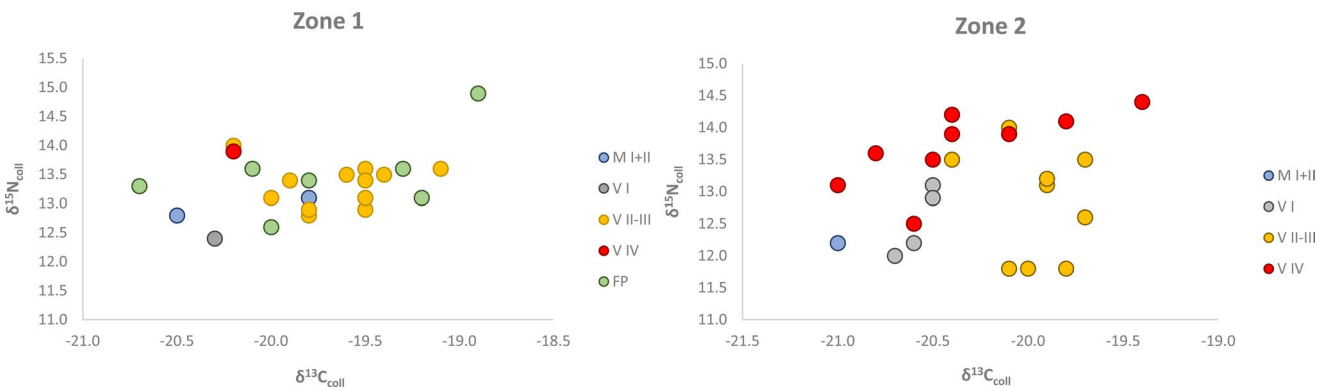

Fig. 9 Comparison of the dietary isotopes within the two food catchment zones predicted by $^{87}Sr/^{86}Sr$ ratios according to individual chronological phases

Early viking age (V I, 800–880 CE)

The transition from the Merovingian period to the Early Viking Age appears subtle in terms of burial customs at Luistari (Lehtosalo-Hilander 1982b: 179). While a small cluster of samples around the mean of the local bioavailable $^{87}Sr/^{86}Sr$ values suggests continuity of the local community, this phase also displays the highest degree of heterogeneity in multi-isotopic evidence. Moreover, it includes the greatest number of outliers, indicating notable childhood mobility with very high offsets between sampled tissues (Fig. 4:B2; 6). This phase thus distinctly exhibits heightened mobility compared to the previous period and even some contemporary sites in the circum-Baltic area (e.g., Ribe, cf. Croix et al. 2020). The values and quantity of outliers may suggest an open recipient-oriented community with a significant influx of incoming individuals. This emergence of a new community during the 9th century builds upon the existing local settlement, incorporating established food catchment areas and means of subsistence of the original settlers. More negative $\delta^{13}C_{coll}$ and $\delta^{13}C_c$ values in both the earliest periods (i.e. Merovingian and Viking I; Supplementary Fig. 5) compared to later ones can be indicative of smaller field plots and theoretically also increased involvement of forest pasture for local livestock (Drucker et al. 2008; Gerling et al. 2017).

The $^{87}Sr/^{86}Sr$ ratios of the non-local individuals exhibit either very high radiogenic values (graves 130, 294, both individuals in grave 295, and 40) or, conversely, some of the lowest values in the dataset (grave 41). The origin of the highly radiogenic samples can highly likely be traced back to Finland. High $^{87}Sr/^{86}Sr$ ratios are associated especially with much of southern Finland, due to the large Rapakivi intrusions and rocks of the prominent schist belts in the region (Kaislaniemi 2011), reflected also in previously reported archaeological faunal samples from these regions (Price et al. 2021). For instance, the major river Kokemäenjoki, 19 km to the northeast of Luistari, draining vast catchments (>27 000 km^2) in southwestern Finland, mainly in the provinces of Häme and Pirkanmaa, has yielded a $^{87}Sr/^{86}Sr$ value of 0.7452 (Löfvendahl et al. 1990). Further, a recent modelling study on the geospatial distribution of bioavailable $^{87}Sr/^{86}Sr$ values over Fennoscandia (Armaroli et al. 2024) is consistent with such high $^{87}Sr/^{86}Sr$ values (>0.736) being most common in southern and southwestern Finland, occurring also along the eastern coast of central Sweden. On the other hand, the lowest strontium values in Luistari are more commonly found in people across northern Europe (Fig. 10). Similar $^{87}Sr/^{86}Sr$ ratios for humans are observed e.g. across the Bothnian Sea in and around the Mälaren region in Sweden (Price et al. 2018; Bäckstrom and Price 2016; Krzewińska et al. 2018). Similar modelled bioavailable values are shown widely across eastern parts of Sweden and other regions of Finland, especially in the east and regions north closer to the Bothnian Bay, should not be excluded either (Armaroli et al. 2024), especially in cases of dietary input from the Baltic Sea (e.g. Lahtinen et al. 2020).

During this time period, there was also a notable increase in Finnish artefacts discovered on the Åland islands (Kivikoski, 1963), along with the emergence of Finnish pottery types (AIII) found in Birka and Uppland, Sweden (Gustin and Wessman 2021: 69; Roslund 2017: 182–186). These findings suggest the spread of Finnish influences to other regions. This phenomenon has been linked to the long-distance fur trade network extending from the Baltic Sea to the Volga-Kama region in Central Russia, where individuals from western Finland likely played a central role as early as the 8th century CE (Callmer 2024). The possibility of an eastern origin for the newcomers can't be categorically excluded based on Sr isotopes as there are practically no comparative data from the east, but it was disregarded in favour of western connections between Western Finland, Eastern Scandinavia and Baltic regions, as the latter are supported by archaeological material from Luistari (Lehtosalo-Hilander 1982a, b, c, 2000). It appears that in the case of Luistari, the newcomers from the West integrated into the expanding local community, upholding traditional methods of land exploitation and the community was likely growing.

Mid- and late viking age (V II-III, 880–1000 CE)

The changes observed at the beginning of the Viking Age are reflected in the Mid- and Late Viking Age, characterised by a dynamic increase of graves, and an abundance of grave goods and rich furnishings, to the extent that the graves dating to this period form a clear, distinctive group (Lehtosalo-Hilander 2000: 228). This period can be viewed as a peak in terms of both socio-economic and population standpoints.

Compared to the preceding period, there is a positive shift in $\delta^{13}C_c$ and $\delta^{13}C_{coll}$ values and, to a certain extent, also $\delta^{15}N_{coll}$ values (Fig. 5:A, Supplementary Figs. 5, 6). This, along with the more consistent strontium isotopic values, suggests a transition in ecological conditions and also in subsistence and agricultural practices, possibly linked to the concurrent amelioration and stabilisation of climatic conditions (e.g. Mann 2009; Helama et al. 2017; Ljungqvist 2010; Etu-Sihvola et al. 2022). Isotopic data show differentiated approaches to various food catchment zones, employing different exploitation patterns in Zone 1 and 2, respectively. Consequently, more stable local economic conditions can be supposed, alongside continued settlements characterised by consistent yet diverse landscape exploitation patterns. This could mean that multiple settlement sites, each with distinct

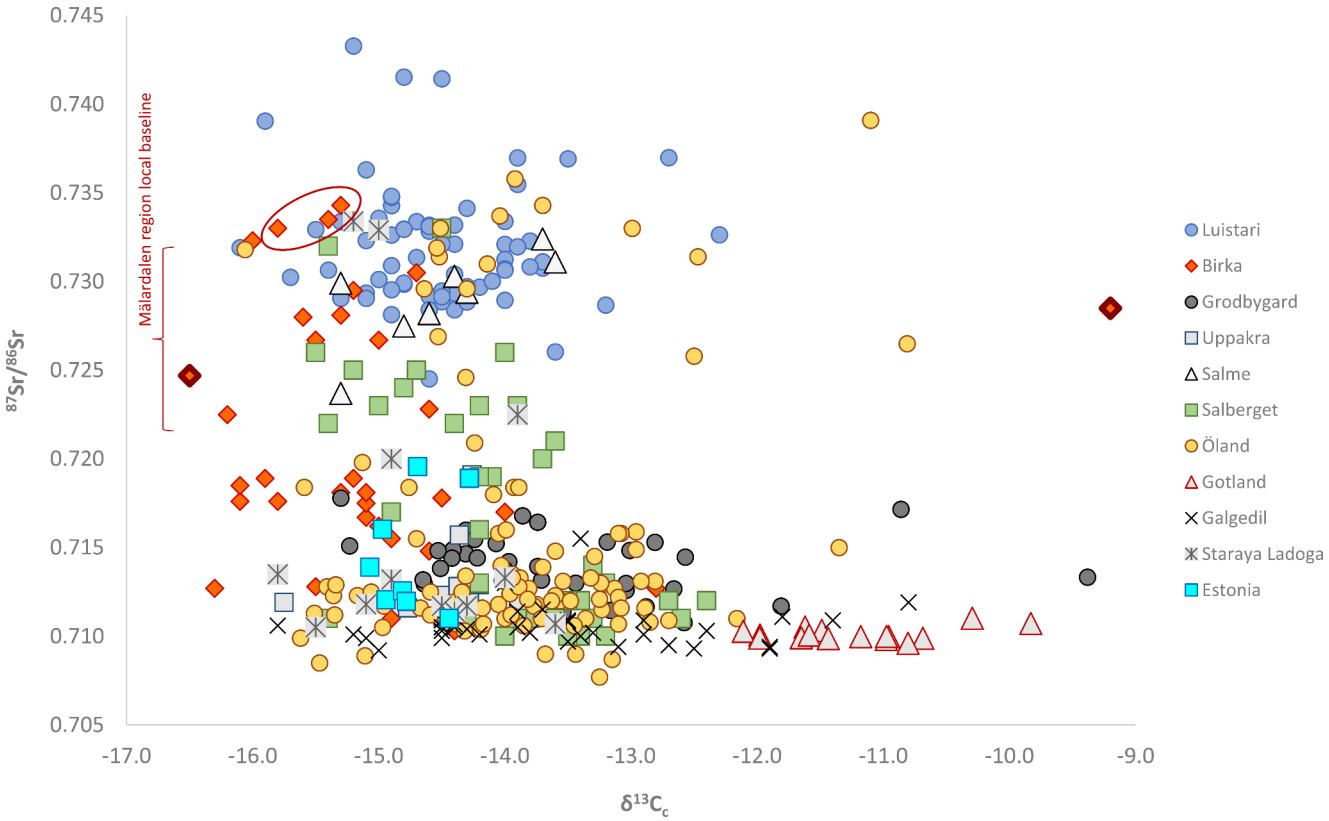

Fig. 10 A comparison of human $^{87}Sr/^{86}Sr$ vs. $\delta^{13}C_c$ values in Luistari and other archeological contexts from the circum-Baltic area, where both Sr and C bioapatite data are available: Gotland/Västerbjers (3000−2600 BCE; Ahlström and Price 2021), Öland island (ca. 500 BCE to 1040 CE; Wilhelmson and Ahlström 2015), Grødbygård/Bornholm Island (11th century CE; Price et al. 2012); Central Sweden-Mälaren region/Salberget (15th century CE; Bäckström and Price 2016); Mälaren region/Birka (ca. 750–975 CE; Price et al. 2018), Saaremaa island/Salme (ca. 750 CE; Price et al. 2016), western Scania, Sweden/Uppåkra (ca. 100 BCE to 1000 CE; Price 2013), Northern Estonia/Ilmandu, Joelähtme, Kunda, Muuksi (ca. 1200−400 BCE; Oras et al. 2016), Karelia (Russia)/Staraja Ladoga (ca. 1000–1100 CE; Price et al. 2019), Funen island, Denmark/Galgedil (ca. 800–1050 CE; Price et al. 2014). Note the extensive temporal span of the presented data. See Fig. 1 for location of sites

patterns of resource and land use, used Luistari as a common burial place.

Both the $^{87}Sr/^{86}Sr$ ratios and the $\delta^{13}C_c$ indicate a relatively homogeneous population across a wider geographical area. Particularly in this period, where the highest number of samples were analysed for the ED statistics, the distinction between individuals clustering around homogeneous values and those whose values are more distant are visible (Supplementary Fig. 6). This can indicate potential differences between the core community and the potential non-locals or individuals with different subsistences.

Furthermore, the data from multiply sampled individuals reveal diverse patterns of childhood mobility and suggest movements within the region and beyond. This is particularly evident in cases such as graves 62, and 1260 (Supplementary Table 3), and it suggests heightened interactions between population groups (communities) within and also beyond the Luistari area, possibly linked to increased population numbers and growing stable socio-economic environment. Moreover, greater social engagements such as marriages, social and economic networks can be inferred, given the more pronounced movements across the area. The isotopic mobility patterns, on the other hand, do not appear to involve more distant areas on a regular basis, and some of the richly furnished graves (such as the female grave 1260) seem to belong to locals.

The viking IV period (V IV, 1000–1070 CE)

The subsequent Viking IV period demonstrates a notably stabilised local community, rooted in previously established subsistence and economic patterns. It is noteworthy that many of the wealthiest and archaeologically distinctive graves are dated to this period. A stable local community with well-established long-distance networks is evident, as the origins of individuals with $\delta^{13}C_c$ and/or $^{87}Sr/^{86}Sr$ values distinct from the core population (Fig. 5:A; graves 56, 290, 359, 480) suggest involvement with more distant areas both within Finland and potentially across the Baltic Sea. Similar to period V I, the lower $^{87}Sr/^{86}Sr$ of the female from the

exceptionally rich grave 359 aligns with values of humans interpreted to originate from the Mälaren region (Fig. 10) (Price et al. 2018; Wilhelmson and Ahlström 2015; Bäckstrom and Price 2016) and bioavailable $^{87}Sr/^{86}Sr$ values modelled for eastern Sweden, but Finland should not be excluded either (Armaroli et al. 2024). The Swedish connection is further supported by the grave goods. Two remaining outstanding individuals are notable for their atypical $\delta^{13}C_c$ values (grave 290 = -15.7‰; grave 480 = -12.3‰). While grave 290 is consistent with the Sr and C isotopes of the Birka assemblage (Fig. 10), the exceptionally high carbon value in combination with the typical Luistari strontium value in the case of grave 480 lacks parallels in the circum-Baltic area. Some values on the island of Öland considered outliers with possible origins in the Mälaren region (Wilhelmson and Ahlström 2015) are similar to this one (Fig. 10).

This period directly follows the abandonment of Birka and the establishment of Sigtuna ca. 980 CE (Roslund 2017: 187–188; Zachrisson 2020: 274). During this period, the contacts between western Finland and eastern Sweden are indicated by mostly female Finnish artefacts found in Sigtuna and its surroundings. It seems that the already established networks that were based on interregional exchange remained even after the eastern fur trade had ceased around 860 CE (Callmer 2024). Comparing the isotopic results with grave goods from Luistari cemetery indeed reveal that local individuals were also actively engaged in transregional interactions. For example, the contents of male grave 480, namely the large penannular brooch with flower-shaped ends shows influences from Baltic countries and Scandinavia (Lehtosalo-Hilander 1982b: 106), as well as the amber bead and Arabic silver coin (Lehtosalo-Hilander 2000: 32) are indicative of an individual with access to a wide range of goods from different regions. Similarly, the rich female grave 1260, which included two Finnish round concave brooches, a bronze chain set, a Baltic type of torc, and strings of beads that follow the female fashion trends in the Baltic countries and Gotland (Bliujienė 2001), provides evidence of local individuals engaging with broader cultural trends. These findings demonstrate the complex and interconnected nature of social and cultural networks during this period, highlighting the cosmopolitanism of Luistari individuals, whether local or non-local.

It is interesting that the outliers who clearly seem to have been newcomers (for example females in graves 56 and 359) cannot be distinguished by their grave-goods or dress accessories. Clothes and costume accessories, especially female, are usually considered strong markers of regional and cultural identities (Kershaw 2013: 157–178; Raffield 2000: 34, 36; Røstad 2021: 34–36), but our results (see also Montgomery et al. 2014 for similar examples from the isles of Orkney and Lewis) indicate that clothing accessories cannot be used as a direct indication of an individual's geographical origins, as in the case of grave 359, where the buried female was clearly non-local, and possibly from outside of Finland, too. Similar cultural integration has previously been observed in Gotland, where newcomers typically had Gotlandic dress accessories in their graves (Raffield 2000: 37). However, the results from grave 56 indicate local mobility within Finland, and therefore, the presence of Western Finnish costume and dress accessories may simply reflect the fact that the individual originated from this cultural area. The overall high female mobility may indicate exogamous practices during the period.

Interestingly, there is a dietary isotopic distinction between this period and the preceding one. Carbon isotope values are visibly more negative in this period, particularly $\delta^{13}C_{coll}$ values (Supplementary Fig. 5). Alongside the visibly higher $\delta^{15}N_{coll}$ values, this may indicate a shift in the protein source of the diet along a trophic level (Hedges and Reynard 2007). Unlike the previous period, a greater reliance on proteins such as meat or lake fish may be inferred. The reasons for this significant change in dietary strategies are challenging to explain; however, increased reliance on hunting or fishing may suggest a decreased dependability on annual crop seasons, among other factors. While the two food catchment zones, consistent with the previous period, remain distinguishable, there is a notable prevalence of samples in Zone 2, indicating distinct settlement and land exploitation preferences with a shift towards more radiogenic areas. Low $\delta^{15}N_{coll}$ values in case of richly furnished graves in this zone may also suggest that despite the changing subsistence conditions, the elite maintained a consistent dietary standard. These findings could suggest socially-driven uneven subsistence patterns, possibly indicative of a larger community with varying dietary preferences or multiple settlements with distinct dietary practices within the same region under possibly changing environmental conditions.

The final period (1070–1130 CE)

In the Final period (1070–1130 CE), a contraction of the $^{87}Sr/^{86}Sr$ values in contrast to the broader spread of $\delta^{13}C_c$ values can be observed. This suggests a geographically restricted food catchment area with less cohesive subsistence strategies and possibly also a smaller community. This could be interpreted as a sign of one community or village but scattered way of subsistence or different field plots for different families or groups. During this period, there are no indications of either short- or long-distance mobility. However, the limited availability of individuals for sampling from this period means that these observations may

be influenced by sample count bias. Nevertheless, the most profound changes in the burial customs occurred during this period. Swords and spearheads were not placed in graves anymore, and knives and firesteel became the most common grave goods in Luistari (Lehtosalo-Hilander 1982b: 183–184). This could indicate wider changes taking place in the community, possibly relating to the spread of Christianity.

Luistari $^{87}Sr/^{86}Sr$ and $\delta^{13}C_c$ in the wider circum-baltic context

Figure 10 compares the Luistari human $^{87}Sr/^{86}Sr$ and $\delta^{13}C_c$ values to those from other archaeological contexts of various ages from the circum-Baltic area (see Fig. 1 for locations). All of the comparative datasets were reported to include non-local individuals, and thus their full distributions should not be taken to reflect typical values of "local" inhabitants at these sites. A notable similarity between the burial population of Luistari and the higher spectrum of the comparative $^{87}Sr/^{86}Sr$ values, the majority of which is reported from Birka in the Mälaren region of eastern Central Sweden (Price et al. 2018) and the island of Öland in the Baltic Sea (Wilhelmson and Ahlström 2015) is observed. In Central Sweden/Mälaren region, local values are considered to range upwards of 0.720 (Salberget) or 0.7230 (Birka), and accordingly, the higher Sr isotope values observed for datasets from Öland, Salme and Staraya Ladoga were considered consistent with bioavailable Sr values in Central Sweden/Mälaren area by the original authors. The considerable overlap of Sr isotope values of the local bioavailable baseline for the Luistari population in southwestern Finland and that in the Central Swedish/Mälaren region effectively precludes distinguishing residency between these two important regions for the Baltic Sea network using $^{87}Sr/^{86}Sr$ alone in the common range of Sr isotope baseline values from 0.726 to 0.733.

At the same time, the distribution of $\delta^{13}C_c$ values for Luistari show considerable similarity with most of the projected comparative sites in Sweden, Estonia and Russian Karelia, the exception being the Neolithic individuals from Västerbjers Gotland, with a high marine influence raising the carbon isotope baseline. Thus, $\delta^{13}C_c$ might not be among the best diagnostic tools for provenancing in this region, with the exception of separating clearly marine influenced (coastal/island) and inland locations. However, if only the individuals interpreted as locals in Birka ($^{87}Sr/^{86}Sr$: 0.723–0.733; Price et al. 2018) are taken into account, the Luistari people show a tendency for higher $\delta^{13}C_c$ values– possibly related to the effects of Satakunta sandstone calcite raising the $\delta^{13}C$ levels of the Pyhäjärvi lake which contributes prominently to diets of the Luistarians (Etu-Sihvola et al. 2022).

The two (Fig. 10, thickly outlined) individuals from the Birka assemblage, that were associated with grave goods interpreted as of Finnish origin (Price et al. 2018), show $^{87}Sr/^{86}Sr$ values on the lower fringe for the Eura region and perhaps southwestern Finland in general factoring in the high $^{87}Sr/^{86}Sr$ values obtained on humans in the Turku region (mean 0.7332; Price et al. 2021). Also their $\delta^{13}C_c$ isotopic values deviate significantly from those that are typical for Luistari in both cases and indeed from the whole dataset available in the Baltic region. They were considered locals to Birka based on their $^{87}Sr/^{86}Sr$ values within the bioavailable range, supporting an observation made above about the geographical non-alignment between the costume parts and persons´ origins. However, as noted earlier, while the burial population sample in Luistari and near Turku show high $^{87}Sr/^{86}Sr$, regions and populations with lower characteristic values do also exist in Finland (e.g. Lahtinen et al. 2020) and are likely to emerge in future research extending to new sites. In the Birka burial population, three individuals (circled in Fig. 10) with high $^{87}Sr/^{86}Sr$ values above the upper limit of the local baseline at 0.733 were tentatively associated with Finland or northern Sweden based on general expectations of high Sr isotope levels (Price et al. 2018). While not at the center of the distribution, their $^{87}Sr/^{86}Sr$ and $\delta^{13}C_c$ levels are compatible with the range of values in Luistari. Furthermore, we note that some of the individuals from the Salme ship burial in Estonia, interpreted to originate from the Mälardalen region (Price et al. 2016) show a higher level of affinity to the Luistari distribution especially with regard to the $\delta^{13}C_c$ values, that tend to be less negative than the values obtained from Birka. An intriguing observation is the difference in $\delta^{13}C_c$ values between locals at Birka and the Öland island incomers with interpreted origins in the Mälaren region (Wilhelmson and Ahlström 2015) within the more radiogenic range of $^{87}Sr/^{86}Sr$ values. These values are possibly influenced by variations in baselines or respective diets at different time periods, but possibly also different origins of the non-local individuals at Öland.

Conclusion

The Luistari burial community provides a unique opportunity to examine subsistence and mobility patterns in Iron Age and Early Medieval Finland. This long-term utilised cemetery likely served as a central burial site for local communities, gathering burials from surrounding settlements. Despite the absence of conclusive evidence for contemporary settlements in the archaeological record, isotopic data indicate the exploitation of two distinct food catchment zones situated in different geological areas. The local communities utilised diverse environments characterised

by both less radiogenic and more radiogenic strontium isotopes. While certain periods exhibit a preference for specific zones, during peak periods (especially periods VII-III), the growing local population adopted various subsistence strategies throughout the region around Pyhäjärvi Lake.

The chronology of the Luistari cemetery spans over five hundred years, during which the local population exhibits diverse mobility patterns. A consistent cluster of individuals conforms to the local bioavailable strontium signal, but the pattern of non-locals changes over time. Notably, the Viking I period marks a significant transformation, with the establishment of a "founding" community comprising the original local population from the Merovingian period, supplemented by newcomers possibly from western Baltic and Scandinavian regions. During periods VII-III (post-9th century AD), a more pronounced shift is observed, characterised by fundamental changes in dietary and migratory patterns. New data suggest that vibrant mobility within Finland, rather than systematic movement across the Baltic Sea, was the focus during this time. In contrast, the subsequent phase (period V IV) reveals both maritime and continental long-distance connections, as the long-established local community integrates into extensive communication networks by the discernible mobility of persons. These non-local individuals likely played significant roles, being associated with political and commercial activities in the circum-Baltic area. These connections likely ceased in the final period, possibly alongside a decrease in the size of the local population. Notably, the early Viking period (V I) and the late Viking period (V IV) exhibit the highest prevalence of distinctly offset values over chronological periods. Conversely, the remaining periods demonstrate a consistent range of $^{87}Sr/^{86}Sr$ values, suggesting varied and less long-distance oriented mobility patterns.

A thorough evaluation of the Luistari isotopic and archaeological dataset underscores the advantage of multi-isotopic evidence in investigating local mobility and socio-economic patterns. Some non-local individuals could not be identified using strontium isotopic values alone. However, by combining with other evidence, notably the $\delta^{13}C_c$ values proved to be invaluable in identifying both locals and non-locals, and the broader mobility and subsistence patterns within the circum-Baltic area (Fig. 10). The inclusion of subsistence isotopes, specifically $\delta^{13}C_{coll}$ and $\delta^{15}N_{coll}$, further enabled the exploration of local subsistence strategies within the regional environment. This analysis supports the hypothesis that several regional settlements utilised Luistari as a communal burial site.

Finally, the statistical methods used for outlier detection and the analysis of internal data structure proved more effective compared to commonly employed statistical techniques. For future studies, it is recommended to utilise multi-isotopic evidence and conduct comprehensive bio-available strontium sampling where and when possible. This approach is most beneficial for the complex evaluation of burial communities.

Supplementary Information The online version contains supplementary material available at https://doi.org/10.1007/s12520-024-02147-6.

Acknowledgements We are very grateful to both reviewers, whose comments have significantly improved the quality of the original manuscript. Hanna Turunen and Igor Shevchuk at the Laboratory of Chronology, Finnish Museum of Natural History, are gratefully acknowledged for their significant contributions to the baseline field studies and sample processing. Kristiina Mannermaa is thanked for her contribution to the archaeological faunal samples and comments on the manuscript. Lukáš Ackerman acknowledges the institutional support through the project RVO67985831. We are grateful to Veronika Renčiuková and Jan Rejšek (both from the Institute of Geology of the Czech Academy of Sciences) for their help with Sr isotopic analyses. Alžběta Danielisová acknowledges the support of the project financed by the Czech Ministry of Education, Youth and Sports, reg. no. CZ.02.01.01/00/22_008/0004593.

Author contributions A.D. - Conceptualisation, Investigation, Formal analysis, Data curation, Writing - original draft, Writing - review & editing, VisualisationU.M. - Investigation, Writing - original draft, Writing - review & editingS.K. - Formal analysis, Writing - original draft, VisualisationA.W. - Writing - review & editingL.Ack. - Investigation, Writing - review & editingM.O. - Writing - review & editingH.E-Si. - Conceptualisation, Investigation, Writing - review & editingL.Arp. - Initiation of the study, Funding acquisition, Conceptualisation, Supervision, Investigation, Formal analysis, Writing - original draft, Writing - review & editing, Visualisation.

Funding Open Access funding provided by University of Helsinki (including Helsinki University Central Hospital).
This study was funded by the Kone Foundation.

Data availability No datasets were generated or analysed during the current study.

Declarations

Competing interests The authors declare no competing interests.

References

Ahlström T, Price TD (2021) Mobile or stationary? An analysis of strontium and carbon isotopes from Västerbjers, Gotland, Sweden. J Archaeol Science: Rep 36:102902

Andreasen R, Thomsen E (2021) Strontium Is Released Rapidly From Agricultural Lime–Implications for Provenance and Migration Studies, Frontiers in Ecology and Evolution 8

Armaroli E, Lugli F, Cipriani A, Tütken T (2024) Spatial ecology of moose in Sweden: Combined Sr-O-C isotope analyses of bone and antler. PLoS ONE 19, e0300867

Bataille CP, Jaouen K, Milano S, Trost M, Steinbrenner S, Crubézy É, Colleter R (2021) Triple sulfur-oxygen-strontium isotopes probabilistic geographic assignment of archaeological remains using a novel sulfur isoscape of western Europe. PLoS ONE 16, e0250383

Bäckström Y, Price TD (2016) Social identity and mobility at a preindustrial mining complex, Sweden. J Archaeol Sci 66:154–168

Beaver JE, Dean RM (2019) Using euclidean distance in the comparative analysis of taxonomic abundance. J Archaeol Science: Rep 25:331–340

Bentley AR (2006) Strontium isotopes from the Earth to the Archaeological Skeleton: a review. J Archaeol Method Theory 13:135–187

Blank M, Sjögren K-G, Knipper C, Frei KM, Storå J (2018) Isotope values of the bioavailable strontium in inland southwestern Sweden—A baseline for mobility studies. PLoS ONE 13, e0204649

Bliujiené A (2001) Curonian bead sets with bronze spacer plates and their scandinavian parallels. Fornvännen 96:235–242

Bryant JD, Froelich PN (1995) A model for oxygen isotope fractionation in body water of large mammals. Geochim Cosmochim Acta 59:4523–4537

Budd P, Millard A, Chenery C, Lucy S, Roberts C (2004) Investigating population movement by stable isotope analysis: a report from Britain. Antiquity 78(299):127–141

Callmer J (2024) Eastern Middle Sweden, Finland, and beyond in the Late Vendel and Early Viking periods. In memory of Professor Ella Kivikoski, Helsingfors (1901–1990), Fornvännen 119(1), 1–24

Croix S, Frei KM, Sindbæk SM, Søvsø M (2020) Individual geographic mobility in a viking-age emporium—burial practices and strontium isotope analyses of Ribe's earliest inhabitants. PLoS ONE 15, e0237850

Daux V, Lécuyer C, Héran M-A, Amiot R, Simon L, Fourel F, Martineau F, Lynnerup N, Reychler H, Escarguel G (2008) Oxygen isotope fractionation between human phosphate and water revisited. J Hum Evol 55:1138–1147

DG Drucker, Bridault A, Hobson KA, Szuma E, Bocherens H (2008) Can carbon-13 in large herbivores reflect the canopy effect in temperate and boreal ecosystems? Evidence from modern and ancient ungulates. Palaeogeogr Palaeoclimatol Palaeoecol 266:69–82

Dudás FÖ, LeBlanc SA, Carter SW, Bowring SA (2016) Pb and Sr concentrations and isotopic compositions in prehistoric north American teeth: a methodological study. Chem Geol 429:21–32

Etu-Sihvola H, Oinonen M, Mizohata K, Onkamo P, Arppe L (in preparation). Timelines of the early Medieval Luistari cemetery (Finland) through radiocarbon and stable isotopic analyses

Etu-Sihvola H, Salo K, Naito YI, Kytökari M, Ohkouchi N, Oinonen M, Heyd V, Arppe L (2022) Isotopic insights into the early medieval (600–1100 CE) diet in the Luistari cemetery at Eura, Finland. Archaeol Anthropol Sci 14:143

Fahy GE, Deter C, Pitfield R, Miszkiewicz JJ, Mahoney P (2017) Bone deep: variation in stable isotope ratios and histomorphometric measurements of bone remodelling within adult humans. J Archaeol Sci 87:10–16

Gerling C, Doppler T, Heyd V, Knipper C, Kuhn T, Lehmann MF, Pike AWG, Schibler J (2017) High-resolution isotopic evidence of specialised cattle herding in the European neolithic. PLoS ONE 12, e0180164

Glykou A, Eriksson G, Storå J, Schmitt M, Kooijman E, Lidén K (2018) Intra- and inter-tooth variation in strontium isotope ratios from prehistoric seals by laser ablation multi-collector inductively coupled plasma mass spectrometry. Rapid Commun Mass Spectrom 32:1215–1224

Greenland S, Senn SJ, Rothman KJ, Carlin JB, Poole C, Goodman SN, Altman DG (2016) Statistical tests, P values, confidence intervals, and power: a guide to misinterpretations. Eur J Epidemiol 31:337–350

Gustin I (2017) Contacts, identity and hybridity: objects from SW Finland in the Birka Graves. In: Callmer J, Roslund M, Gustin I (eds) Identity formation and diversity in the early medieval Baltic and Beyond. Communicators and communication. Leiden, Brill, pp 205–258

Gustin I, Wessman A (2021) Western Finland in the viking world. In: Aannestad HL, Pedersen U, Moen M, Naumann E, Lund Berg H (eds) Vikings across Boundaries. Viking-age transformations. Volume II. Routledge, pp 60–79

Hedges REM, Reynard LM (2007) Nitrogen isotopes and the trophic level of humans in archaeology. J Archaeol Sci 34:1240–1251

Helama S, Jones PD, Briffa KR (2017) Dark Ages Cold Period: a literature review and directions for future research. Holocene 27:1600–1606

Hennius A (2021) *Outlanders? Resource colonisation, raw material exploitation and networks in Middle Iron Age Sweden*. PhD thesis. University of Uppsala

Holt E, Evans JA, Madgwick R (2021) Strontium (87Sr/86Sr) mapping: a critical review of methods and approaches. Earth Sci Rev 216:103593

Hrnčíř V, Laffoon JE (2019) Childhood mobility revealed by strontium isotope analysis: a review of the multiple tooth sampling approach. Archaeol Anthropol Sci 11:5301–5316

Kaislaniemi L (2011) Estimating the distribution of strontium isotope ratios (87 Sr / 86 Sr) in the Precambrian of Finland. Bull Geol Soc Finl 83:95–113

Kershaw J, F (2013) Brooch use, culture, and gender. Viking identities: scandinavian jewellery in England. Oxford University Press, Oxford

Kirkinen T, Vajanto K, Björklund S (2020) Animal-hair evidence in an 11th century female grave in Luistari, Finland. Archaeol Text Rev 6:109–125

Kivikoski E (1937) Studien zu Birkas Handel Im östlichen Ostseegebiet. Acta Archaeologica VIII:229–250

Kivikoski E (1963) Kvarnbacken. Ein Gräberfeld der jüngerenEisenzeit auf Åland. Helsinki: SMY

Kivikoski E (1964) Finlands förhistoria. Almqvist & Wiksell, Stockholm

Knipper C, Koncz I, Ódor JG, Mende BG, Rácz Z, Kraus S, van Gyseghem R, Friedrich R, Vida T (2020) Coalescing traditions—coalescing people: community formation in Pannonia after the decline of the Roman Empire. PLoS ONE 15, e0231760

Knipper C, Pichler SL, Brönnimann D, Rissanen H, Rosner M, Spichtig N, Stopp B, Rentzel P, Röder B, Schibler J, Lassau G, Alt KW (2018) A knot in a network: residential mobility at the Late Iron Age proto-urban centre of Basel-Gasfabrik (Switzerland) revealed by isotope analyses. J Archaeol Science: Rep 17:735–753

Kohonen J, Pihlaja P, Kujala H, Marmo J (1993) Sedimentation of the Jotnian Satakunta sandstone, western Finland. Geological Survey of Finland, Bulletin 369, 35 pp

Kootker LM, Laffoon JE (2020) Assessing the preservation of biogenic strontium isotope ratios (87Sr/86 Sr) in the pars petrosa

ossis temporalis of unburnt human skeletal remains: a case study from Saba. Rapid Commun Mass Spectrom 36(10):e9277
Kortelainen N, Karhu J (2009) Geochemical and isotopic evaluation of high-pH groundwater in a carbonate-bearing glacigenic aquifer, SW Finland. Hydrol Res 40:19–31
Kortelainen NM, Korkeakoski PJ, Karhu JA (2007) Origin of calcite in the glacigenic Virttaankangas complex. Bull Geol Soc Finl 79:5–15
Krueger HW, Sullivan CH (1984) Models for carbon isotope fractionation between diet and bone. In: Turnlund, J.R. and Johnson, P.E. (Eds.), Stable isotopes in nutrition, Vol. 258. ACS symposium series, American Chemical Society, pp. 205–220
Kruschke J, K (2015) Doing bayesian data analysis: a tutorial with R, JAGS, and Stan. Edition 2. Academic, Boston
Krzewińska M, Kjellström A, Günther T, Hedenstierna-Jonson C, Zachrisson T, Omrak A, Yaka R, Kılınç GM, Somel M, Sobrado V, Evans J, Knipper C, Jakobsson M, Storå J, Götherström A (2018) Genomic and Strontium Isotope Variation Reveal Immigration Patterns in a Viking Age Town, Current Biology 28:2730–2738.e2710 https://doi.org/10.1016/j.cub.2018.06.053.
Ladegaard-Pedersen P, Sabatini S, Frei R, Kristiansen K, Frei KM (2021) Testing late bronze age mobility in southern Sweden in the light of a new multi-proxy strontium isotope baseline of Scania. PLoS ONE 16, e0250279
Laffranchi Z, Granados-Torres A, Lösch S, Zink A, Dori I, Delgado-Huertas A, Milella M (2022) Celts up and down the Alps. Insights on mobility patterns in the pre-Roman/Celtic population from Verona (NE Italy, 3rd–1st c. BCE): a multi-isotopic approach. Am J Biol Anthropol 178:513–529
Lahtinen M, Arppe L, Nowell G (2020) Source of strontium in archaeological mobility studies—marine diet contribution to the isotopic composition. Archaeol Anthropol Sci 13:1
Lee-Thorp JA, Sealy JC, van der Merwe NJ (1989) Stable Carbon isotope ratio differences between bone collagen and bone apatite, and their relationship to diet. J Archaeol Sci 16:585–599
Lehtinen M, Nurmi PA, Rämö OT (eds) (2005) Precambrian geology of Finland– key to the evolution of the fennoscandian shield. Elsevier B.V., Amsterdam, p 236
Lehtosalo-Hilander P-L (1982a) Luistari I– The Graves. Suomen Muinaismuistoyhdistyksen Aikakauskirja, 82:1. Helsinki: Finnish Antiquarian Society
Lehtosalo-Hilander P-L (1982b) Luistari II– the artefacts. Suomen Muinaismuistoyhdistyksen Aikakauskirja, 82:3. Helsinki: Finnish Antiquarian Society
Lehtosalo-Hilander P-L (1982c) Luistari III– A Burial-Ground Reflecting the Finnish Viking Age Society. *Suomen Muinaismuistoyhdistyksen Aikakauskirja* 82:3. Helsinki: Finnish Antiquarian Society
Lehtosalo-Hilander P-L (1983) Gutarnas förbindelser med Finland. In: Jansson I (ed) Gutar och vikingar. Statens Historiska Museum, Stockholm, pp 288–305
Lehtosalo-Hilander P-L (2000) Luistari - A history of weapons and ornaments. Luistari IV. *Suomen Muinaismuistoyhdistyksen Aikakauskirja* 107. Helsinki: Finnish Antiquarian Society
Lengfelder F, Grupe G, Stallauer A, Huth R, Söllner F (2019) Modelling strontium isotopes in past biospheres– Assessment of bioavailable 87Sr/86Sr ratios in local archaeological vertebrates based on environmental signatures. Sci Total Environ 648:236–252
Löfvendahl R, Åberg G, Hamilton PJ (1990) Strontium in rivers of the Baltic Basin. Aquat Sci 52:316–333
Lightfoot E, O'Connell TC (2016) On the Use of Biomineral Oxygen Isotope Data to Identify Human Migrants in the Archaeological Record: Intra-Sample Variation, Statistical Methods and Geographical Considerations. PLoS ONE 11, e0153850
Ljungqvist FC (2010) A new reconstruction of temperature variability in the extra-tropical northern hemisphere during the last two millennia. Geogr Ann 92 A:339–351
Luz B, Kolodny Y, Horowitz M (1984) Fractionation of oxygen isotopes between mammalian bone-phosphate and environmental drinking water. Geochim Cosmochim Acta 48:1689–1693
Mann ME, Zhang Z, Rutherford S, Bradley RS, Hughes MK, Shindell D, Ni F (2009) Global signatures and dynamical origins of the little ice age and medieval climate anomaly. Science 326:1256–1260
Martin JE, Tacail T, Balter V (2017) Non-traditional isotope perspectives in vertebrate palaeobiology. Palaeontology 60:485–502
Maurer A-F, Galer SJ, Knipper C, Beierlein L, Nunn EV, Peters D, Tütken T, Alt KW, Schöne BR (2012) Bioavailable 87Sr/86Sr in different environmental samples—effects of anthropogenic contamination and implications for isoscapes in past migration studies. Sci Total Environ 433:216–229
Montgomery J (2010) Passports from the past: investigating human dispersals using strontium isotope analysis of tooth enamel. Ann Hum Biol 37:325–346
Montgomery J, Grimes V, Buckberry J, Evans J, Richards M, Barrett J (2014) Finding Vikings with Isotope Analysis: the View from Wet and Windy islands. J North Atl Special Volume 7:54–70. https://doi.org/10.3721/037.002.sp705
Nironen M (2017) Guide to the Geological Map of Finland - Bedrock 1:1000000. Geological Survey of Finland, Special Paper 60, 41–76. Geological Survey of Finland, Espoo
Oras E, Lang V, Rannamäe E, Varul L, Konsa M, Limbo-Simovart J, Vedru G, Laneman M, Malve M, Price DT (2016) Tracing prehistoric migration: isotope analysis of bronze age and pre-roman Iron age coastal burials in Estonia. Est J Archaeol 20:3–32
Pin C, Gannoun A, Dupont A (2014) Rapid, simultaneous separation of Sr, Pb, and nd by extraction chromatography prior to isotope ratios determination by TIMS and MC-ICP-MS. J Anal Spectrom 29:1858–1870
Pinhasi R, Fernandes D, Sirak K et al (2015) Optimal ancient DNA yields from the inner ear part of the human petrous bone. PLoS ONE. 2015;10(6):e0129102
Price TD (2013) Human Mobility at Uppåkra. A Preliminary Report on Isotopic Proveniencing. In. Hårdh, B., Larsson, L. (Eds.). Folk, fä och fynd. Acta Archaeologica Lundensia. Series in 8°; Vol. 64, 163–175
Price TD, Arcini C, Gustin I, Drenzel L, Kalmring S (2018) Isotopes and human burials at Viking Age Birka and the Mälaren region, east central Sweden. J Anthropol Archaeol 49:19–38
Price TD, Bläuer A, Oras E, Ruohonen J (2021) Baseline $^{87}Sr/^{86}Sr$ values in Southern Finland and Isotopic Proveniencing of the cemetery at Ravattula Ristimäki. Fennoscandia Archaeologica 28:135–152
Price TD, Burton JH, Bentley RA (2002) The characterization of biologically available strontium isotope ratios for the study of prehistoric Migration. Archaeometry 44:117–135
Price TD, Moiseyev V, Grigoreva N (2019) Vikings in Russia: origins of the medieval inhabitants of Staraya Ladoga. Arcaheological Anthropol Sci 11:6093–6109
Price TD, Naum M, Bennike P, Lynnerup N, Frei KM, Wagnkilde H, Pind T, Nielsen FO (2012) Isotopic investigation of human provenience at the eleventh century cemetery of ndr. Grødbygård, Bornholm, Denmark. Dan J Archaeol 1:93–112
Price TD, Prangsgaard K, Kanstrup M, Bennike P, Frei KM (2014) Galgedil: isotopic studies of a viking cemetery on the Danish island of Funen, AD 800–1050. Dan J Archaeol 3:129–144
Price T, Peets J, Allmäe R, Maldre L, Oras E (2016) Isotopic provenancing of the Salme ship burials in pre-viking Age Estonia. Antiquity 90(352):1022–1037

Raffield B (2020) No one is an island: in-group identities in the Viking-Age Baltic. In: Kitzler L, Åhfeldt C, Hedenstierna-Jonson P, Widerström, Raffield B (eds) Relations and runes: the Baltic Islands and their interactions during the Late Iron Age and Early Middle ages. The Swedish National Heritage Board, Stockholm, pp 31–40

Raninen S, Wessman A (2015) Rautakausi. In: G. Haggrén, P. Halinen, M. Lavento, S. Raninen & A. Wessman (eds.), *Muinaisuutemme jäljet. Suomen esi- ja varhaishistoria kivikaudelta keskiajalle*. Gaudeamus, pp. 215–365

Reynard B, Balter V (2014) Trace elements and their isotopes in bones and teeth: Diet, environments, diagenesis, and dating of archeological and paleontological samples. Palaeogeogr Palaeoclimatol Palaeoecol 416:4–16

Roslund M (2017) Bringing the periphery into Focus: Social Interaction betweenBaltic finns and the Svear in the viking age and crusade period (c.800 to 1200). In: Callmer J, Roslund M, Gustin I (eds) Identity formation and diversity in the early medieval Baltic and Beyond. Communicators and communication. Leiden, Brill, pp 168–204

Røstad I (2021) The Language of Jewellery. Dress-accessories and negotiations of identity in Scandinavia, c. AD 400–650/700. Cappelen Damm Akademisk: Oslo

Sahlstedt E, Arppe L (2020) Sequential extraction of the phosphate and collagen fractions of small bone samples for analysis of multiple isotope systems (δ 18 O PO4, δ 13 C, δ 15 N). Rapid Commun Mass Spectrom 34, e8877

Scheeres M, Knipper C, Hauschild M, Schönfelder M, Siebel W, Pare C, Alt KW (2014) Celtic migrations: fact or fiction? Strontium and oxygen isotope analysis of the Czech cemeteries of Radovesice and Kutná Hora in Bohemia. Am J Phys Anthropol 155:496–512

Sheather SJ, Jones MC (1991) A Reliable Data-based Bandwidth Selection Method for Kernel Density Estimation. J Royal Stat Soc Ser B (Methodological) 53:683–690

Sindbæk S, Arthur P (2008) Trade and exchange. In: Graham-Campbell J, Valor M (eds) The archaeology of medieval Europe. Aarhus University, Aarhus, pp 289–315. Acta Jutlandica, 83:1; Humanities Series 79

Sjögren K-G, Price TD, Kristiansen K (2016) Diet and mobility in the corded ware of central Europe. PLOS ONE 11 e0155083. https://doi.org/10.1371/journal.pone.0155083.

Stene K, Wangen V (2017) The uplands: the deepest of forests and the highest of mountains - resource exploitation and landscape management in the viking age and early Middle ages in southern Norway. In: Glørstad Z, Loftsgarden K (eds) Viking-age transformations. Trade, Craft and resources in Western Scandinavia. Routledge

SYKE/CORINE Land cover (2012) http://paikkatieto.ymparisto.fi/value/, downloaded 22.4.2024

Szostek K, Czech K, Cienkosz-Stepańczak B (2015) Strontium isotopes as an indicator of human migration: easy questions, difficult answers. Anthropol Rev 78

Tsutaya T, Yoneda M (2015) Reconstruction of breastfeeding and weaning practices using stable isotope and trace element analyses: a review. Am J Phys Anthropol 156:2–21

Vaasjoki M (1977) Rapakivi granites and other postorogenic rocks in Finland: their age and the lead isotopic composition of certain associated galena mineralizations. Geological Survey of Finland, Bulletin 294, 64 pp

Vaiglova P, Lazar NA, Stroud EA, Loftus E, Makarewicz CA (2023) Best practices for selecting samples, analyzing data, and publishing results in isotope archaeology. Quatern Int 650:86–100

Varo P (1982) Strontium in Finnish foods. Int J Vitam Nutr Res 52:342–350

Velte M, Czermak A, Grigat A, Haas-Gebhard B, Gairhos A, Toncala A, Trautmann B, Haberstroh J, Päffgen B, von Heyking K, Lösch S, Burger J, Harbeck M (2023) Between Raetia Secunda and the dutchy of Bavaria: exploring patterns of human movement and diet. PLoS ONE 18, e0283243

Veselka B, Locher H, de Groot JCMJ, Davies GR, Snoeck C, Kootker LM (2021) Strontium isotope ratios related to childhood mobility: revisiting sampling strategies of the calcined human pars petrosa ossis temporalis. Rapid Commun Mass Spectrom 35, e9038

Wickham H (2016) Data analysis, Springer

Wiedemann-Bidlack FB, Colman AS, Fogel ML (2008) Phosphate oxygen isotope analysis on microsamples of bioapatite: removal of organic contamination and minimization of sample size. Rapid Commun Mass Spectrom 22:1807–1816

Wilhelmson H, Ahlström T (2015) Iron Age migration on the island of Öland: apportionment of strontium by means of bayesian mixing analysis. J Archaeol Sci 64:30–45

Zachrisson T (2020) Sigtuna: An urban Hub in the Viking World, and its Roots. In: A. Pedersen & S. Sindbæk (eds.), *Viking Encounters: proceedings of the eighteenth Viking Congress, Denmark, August 6–12, 2017*. Århus: Aarhus University Press, pp. 268–285

Žák K, Skála R, Řanda Z, Mizera J, Heissig K, Ackerman L, Ďurišová J, Jonášová Š, Kameník J, Magna T (2016) Chemistry of Tertiary sediments in the surroundings of the Ries impact structure and moldavite formation revisited. Geochim Cosmochim Acta 179:287–311